



1 **Reanalysis of and attribution to near-surface ozone**
2 **concentrations in Sweden during 1990-2013**

3

4 **Camilla Andersson¹, Heléne Alpfjord¹, Lennart Robertson¹, Per Erik Karlsson²**
5 **and Magnuz Engardt¹**

6 [1]{Swedish Meteorological and Hydrological Institute, SE-60176 Norrköping, Sweden}

7 [2]{Swedish Environmental Research Institute, P.O. Box 53021, SE-40014 Gothenburg,
8 Sweden}

9 Correspondence to: C. Andersson (camilla.andersson@smhi.se)

10

11 **Abstract**

12 We have constructed two data sets of hourly resolution reanalyzed near-surface ozone (O₃)
13 concentrations for the period 1990-2013 for Sweden. Long-term simulations from a
14 chemistry-transport model (CTM) covering Europe were combined with hourly ozone
15 concentration observations at Swedish and Norwegian background measurement sites using
16 data assimilation. The reanalysis data sets show improved performance than the original CTM
17 when compared to independent observations.

18 In one of the reanalyses we included all available hourly near-surface O₃ observations, whilst
19 in the other we carefully selected time-consistent observations in order to avoid introducing
20 artificial trends. Based on the second reanalysis we investigated statistical aspects of the near-
21 surface O₃ concentration, focusing on the linear trend over the 24 year period. We show that
22 high near-surface O₃ concentrations are decreasing and low O₃ concentrations are increasing,
23 which is mirrored by observed improvement of many health and vegetation indices (apart
24 from those with a low threshold).

25 Using the chemistry-transport model we also conducted sensitivity simulations to quantify the
26 causes of the observed change, focusing on three processes: change in hemispheric
27 background, meteorology and anthropogenic emissions (Swedish and other European). The
28 rising low concentrations of near-surface O₃ in Sweden are caused by a combination of all



1 three processes, whilst the decrease in the highest O₃ concentrations is caused by O₃ precursor
2 emissions reductions.

3 While studying the relative impact of anthropogenic emissions changes, we identified
4 systematic differences in the modelled trend compared to observations that must be caused by
5 incorrect trends in the utilised emissions inventory or by too high sensitivity of our model to
6 emissions changes.

7

8 **1 Introduction**

9 Elevated concentrations of near-surface ozone (O₃) are a major policy concern, given their
10 ability to damage both vegetation (e.g. Royal Society, 2008) and human health (e.g. WHO,
11 2006). It is also an important greenhouse gas (e.g. IPCC, 2013). Elevated O₃ concentrations
12 are formed in the troposphere by the oxidation of volatile organic compounds (VOCs) and
13 carbon monoxide, driven by solar radiation in a polluted air mixture that includes nitrogen
14 oxides (NO_x). Close to combustion sources, the background O₃ concentration is reduced
15 through reactions with directly emitted nitric oxide (NO; see for example Finlayson-Pitts and
16 Pitts, 2000). However, further away from the source and with sufficient availability of VOCs
17 and the right weather conditions, these NO_x emissions can lead to rises in the O₃
18 concentration. O₃ can be transported to regions far away from the area where it was formed
19 and even across continents (e.g. Akimoto, 2003; Derwent et al. 2015). Oxidized nitrogen can
20 also be transported to remote regions as reservoir species, such as peroxy-acetyl nitrates
21 (PANs). These can be a significant source of NO_x and alongside naturally emitted biogenic
22 VOCs cause O₃ formation in otherwise non-polluted areas (e.g. Jacob et al., 1993).

23 European and North American anthropogenic emissions of NO_x increased over most of the
24 20th century, but decreased strongly since the 1980s due to emission control (e.g. Lamarque et
25 al., 2010; Granier et al., 2011). Asian emissions have continued to rise under the same period
26 (Ohara et al., 2007). Jonson et al. (2006) showed that the trend in O₃ concentration in Europe
27 cannot be fully explained by changes in European precursor emissions. By inter-continental
28 transport the increasing precursor emissions in Asia could contribute to increasing
29 background levels with at least a strong impact in North America (Vestraeten et al., 2015),
30 whilst the trend in European background O₃ seasonal variation could also be affected by the
31 decreases in North American precursor emissions (Derwent et al., 2015). Climate also
32 changes over time, causing both changes to the O₃ forming potential, biogenic emissions of



1 O₃ precursors and deposition processes (Andersson and Engardt, 2010). Variability in climate,
2 such as the North Atlantic Oscillation (NAO), contributes to the variation in O₃ concentration
3 in the upper troposphere through variations both in the stratospheric contribution and in the
4 transport patterns (Gaudel et al., 2015). Although the stratospheric contribution to the O₃
5 concentration at the surface is generally small (3-5 ppb(v)) in Europe (Lelieveld and
6 Dentener, 2000), it can be a relevant contribution to near-surface O₃ in certain areas and time
7 periods (Zanis et al., 2014) and could affect the observed trend in near-surface O₃ (e.g. Fusco
8 and Logan, 2003). Despite the large number of studies of tropospheric O₃, a number of
9 challenges still remain, such as explaining the near-surface concentration trends (Monks et al.,
10 2015).

11 Observations in the northern mid-latitudes, either at the surface (Oltmans et al, 2006) or from
12 ozone-sondes and commercial aircraft (Logan et al., 2012), present the picture of increasing
13 tropospheric O₃ concentrations during the second half of the 20th century (Parrish et al., 2012;
14 Cooper et al., 2014). The strong increase in near-surface O₃ concentration until the late 1990s
15 at three widely separated North Atlantic sites, including Mace Head, seems to have peaked or
16 remained stationary (Simmonds et al 2004; Oltmans et al., 2006; Derwent et al., 2007). At
17 Pico Mountain Observatory in the Azores, a decreasing O₃ concentration trend was observed
18 during 2001-2011 which was believed to be mainly caused by decreasing precursor emissions
19 in North America (Kumar et al., 2013). Air masses with European origin observed at Mace
20 Head show a decrease in summertime peak O₃ concentrations and increase in wintertime,
21 which is believed to be connected to European NO_x policy (Derwent et al., 2013). O₃
22 concentrations observed at European alpine sites and in ozone-sonde data (MOZAIC) above
23 European cities have decreased since 1998 with the strongest decrease in summer (Logan et
24 al., 2012).

25 Several modelling efforts have been conducted to describe the past near-surface O₃
26 concentration development (e.g. Fusco and Logan, 2003; Schultz et al., 2007; Pozzoli et al.,
27 2011, Xing et al. 2015). Parrish et al. (2014) present past trends in tropospheric O₃
28 concentrations modelled with three chemistry-climate models and conclude that while there is
29 considerable qualitative agreement between the measurements and the models, there are also
30 substantial and consistent quantitative disagreements. These include that the models capture
31 only 50 % of the change observed during the last 5-6 decades and little of the observed
32 seasonal differences, and that the rate of the trends are badly captured. There are ways



1 forward to improve the description of the trends: 1) understanding the processes and
2 improving the model description of the physics and chemistry for processes of greatest
3 importance in these models, 2) improving the input data quality and 3) incorporating
4 observations in the model by data fusion methods to accurately represent the past statistics in
5 a reanalysis. The first two are important for conducting scenario calculations, whilst the last
6 is an option for producing mappings.

7 If correctly conducted, data fusion will improve the modelled estimates. If temporal and
8 spatial consistency is not considered, it may however introduce artificial trends. Data
9 assimilation, a subset to data fusion (Zhang et al., 2012), is the process by which observations
10 of a system are incorporated into the model state of a numerical model, in this case into the
11 chemistry transport model (CTM) (Kalnay, 2003; Denby and Spangl, 2010). Advanced data
12 assimilation schemes like the 4 dimensional variational (4dvar; e.g. Courtier et al., 1994;
13 Inness et al., 2013) technique utilize information provided by satellites and propagate this in
14 space and time from a limited number to a wide range of chemical components to provide
15 fields that are physically and chemically consistent with the observations. Inness et al. (2013)
16 performed a reanalysis of global chemical composition, including O₃ concentration, for 2003-
17 2010 using advanced data assimilation of satellite observations within the framework of the
18 monitoring atmospheric composition and climate (MACC) project. They demonstrated
19 improved O₃ and CO concentration profiles for the free troposphere, but biases remained for
20 the lower troposphere. Another global reanalysis using data assimilation of satellite data for
21 2005-2012, showed improved performance for chemical species (Miyazaki et al., 2015) but
22 for the O₃ concentration at the surface errors remain associated with low retrieval sensitivity
23 in the lower troposphere and gaps in spatial representation between the model and
24 observations. In order to improve surface characteristics, in situ observations of O₃ need to be
25 included in data assimilation. Another reanalysis of near-surface O₃ concentration in Europe
26 was conducted for the period 2003-2012 within the MACC project (Katragkou et al., 2015).
27 The reanalysis was based on the MACC global model, which consists of the European Centre
28 for Medium-Range Weather Forecasts' Integrated Forecast System (IFS) coupled to the
29 MOZART-3 CTM. In this reanalysis 4dvar data assimilation was used to incorporate in situ
30 measurement from the databases EMEP and Airbase. The data assimilation reduced the bias
31 in near-surface O₃ concentration in most of Europe, and it reproduced the summertime
32 maximum in most parts of Europe, but not the early spring peak in northern Europe. When
33 restricting the observations to in situ measurements in Europe, the beginning of the time



1 period of the reanalysis can be extended further back in time utilizing simpler data
2 assimilation techniques than 4dvar. Variational analysis in 2 dimensions (2dvar) and the
3 analytical counterpart optical interpolation can be used as a CPU-efficient diagnostic tools to
4 improve modelled near-surface O₃ retrospectively (e.g. Alpfjord and Andersson, 2015;
5 Robichaud and Ménard, 2014).

6 The MATCH (Multi-scale Atmospheric Transport and CHEmistry) Sweden system (Alpfjord
7 and Andersson, 2015) includes an operational CTM and methods for data assimilation of
8 atmospheric concentrations in air and precipitation. The system is used for annual
9 assessments of the near-surface O₃, SO₂, NH₃ and NO₂ background concentrations and
10 deposition of nitrogen, sulfur and base cations in Sweden. In this study, the MATCH Sweden
11 system is used to conduct a reanalysis of the hourly near-surface O₃ concentration for Sweden
12 and Norway during the 24-year period 1990-2013 using 2dvar. We use time-consistent input
13 data to avoid the introduction of artificial trends in the results. In an attempt to understand the
14 trends, we perform model sensitivity analyses and apply the CTM without data assimilation.
15 This approach brings new knowledge to explain the trends in O₃ concentrations found in
16 Sweden.

17 The aims of this study are:

- 18 - To create a state-of-the art long-term, temporally and spatially consistent, reanalysis of
19 hourly near-surface O₃ concentrations covering the geographical areas of Sweden and
20 Norway (see Sect. 2)
- 21 - To evaluate the performance of the O₃ reanalysis of the MATCH Sweden system, used
22 in the annual assessment of air quality in Sweden (see Sect. 3.1)
- 23 - To investigate trends and extreme values in near-surface O₃ in Sweden (see Sect. 3.2)
24 and its implications on health and vegetation (see Sect. 3.4)
- 25 - To understand the causes of the change over time, focusing on contributions of
26 emission change, lateral and upper boundary and meteorological variability. (see Sect.
27 3.3)

28



1 **2 Method**

2 In this study we utilize data assimilation in order to combine the respective best qualities of
3 both a CTM and long-term measurements to map near-surface O₃ concentrations during a
4 long historical time period (1990-2013). We focus our study on Sweden, but also include
5 Norway in the data assimilation.

6 For the data assimilation we use the MATCH Sweden system, which is briefly explained in
7 Sect. 2.1. Here variational analysis in two dimensions is applied, and further details are given
8 in Sect. 2.4. Concentration fields provided by the CTM at each grid point are considered as
9 the “first guess” (background field/prior information) of our “best estimate” of the state of the
10 atmosphere before the introduction of observations (Kalnay, 2003). The method used for the
11 production of the “first guess” is explained in Sect. 2.2. The selection of measurements that
12 are included in the data assimilation is important, both to avoid artificial trends in the
13 reanalysis data and in order to select observation sites with corresponding spatial and
14 temporal representations as in the model. We explain our method for the selection of
15 measurements in Sect. 2.3.

16 One aim of this study is to investigate trends in near-surface O₃ in Sweden. To understand the
17 long-term changes in concentration we try to quantify the causes of change, through model
18 sensitivity analyses, and applying the MATCH model without data assimilation. We
19 investigate the respective contributions to the trends of change in European emissions by
20 separating the impact on O₃ trends of changes in local emissions in Sweden, in hemispheric
21 background concentrations (including changes to the top and lateral boundaries) and in
22 meteorology (including changes to biogenic emissions, transport, O₃ forming capacity, O₃
23 deposition etc.). The method for this quantification is described in Sect. 2.5. The methods we
24 use for evaluation are given in Sect. 2.6.

25

26 **2.1 The MATCH Sweden system**

27 The MATCH Sweden system is an operational system used for annual assessments of near-
28 surface regional background concentrations in air of O₃, NO₂, NH₃ and SO₂ as well as
29 deposition of sulfur, nitrogen and base cations over Sweden (Alpfjord and Andersson, 2015).
30 The system includes an operational CTM (MATCH; Multi-scale Atmospheric Transport and
31 Chemistry; Robertson et al., 1999) and methods for data assimilation (using 2dvar) of



1 atmospheric concentrations in air and precipitation. The yearly results from the mapping can
2 be found at www.smhi.se/klimatdata/miljo/atmosfarskemi.

3 The flow-chart in Fig. 1 describes the parts of the MATCH Sweden system that are used in
4 this reanalysis of near-surface O₃ concentrations. Explanations are provided in Sect. 2.2 to
5 2.4. For a description of the whole MATCH Sweden system, see e.g. Alpfjord and Andersson
6 (2015).

7

8 **2.2 First guess – model assessment**

9 The starting point (cf. Fig. 1) for the two-dimensional variational data assimilation of near-
10 surface O₃ is hourly fields of modelled O₃, produced by MATCH. The MATCH model
11 includes ozone- and particle-forming photo-chemistry with ~60 species (Langner et al., 1998;
12 Andersson et al., 2007, 2015). Part of the gas-phase chemical scheme was updated based on
13 Simpson et al. (2012), except for some reaction rates (following the recommendations by the
14 International Union of Pure and Applied Chemistry, IUPAC), and the isoprene chemistry
15 mechanism that was based on an adapted version of the Carter one-product mechanism
16 (Carter, 1996; Langner et al., 1998). A selection of compounds with different ozone forming
17 potentials is used to represent all hydrocarbons emitted into the atmosphere. The photolysis
18 rates depend on the photolytically active radiation, which is dependent on latitude, time of
19 day, cloud cover etc. In this study MATCH interpolates the input meteorology to a domain
20 covering Europe and surrounding areas with 44 km grid point spacing. MATCH uses all
21 meteorological model layers for vertical wind calculations, but restricts the calculations of
22 chemistry and transport to the lower troposphere using the vertical levels of the
23 meteorological model from the surface up to ca 5 km height.

24 MATCH is an offline model, thus, driven by meteorological data generated externally and as
25 such it is often a challenge to undertake long (multi-decadal) simulations due to non-
26 homogenous input data. Dynamical meteorological models, which provide the three-
27 dimensional meteorology for the offline CTMs, are constantly updated to higher resolutions
28 and more advanced physical schemes. Emission inventories are typically constructed for
29 certain target years and different methods may have been used to compile total emissions
30 and/or the geographical distribution of the emissions. Careless combination of different
31 emission data or meteorology from varying model configurations can introduce artificial



1 secular trends in the modelling of atmospheric pollutants. Emissions of biogenic isoprene are
2 calculated online in MATCH following the E-94 isoprene emission methodology proposed by
3 Simpson et al. (1995). Further details of MATCH in the present model version and its ability
4 to simulate near-surface O₃ can be found in separate publications, for example Markakis et al.
5 (2016), Lacressoniere et al. (2016) and Watson et al. (2015; 2016). In this study, we
6 specifically aimed for internally coherent input data, although it led to compromises in e.g.
7 the temporal coverage of the meteorology and the resolution of the gridded pan-European
8 emissions. In the following sections we briefly describe the utilized input data.

9

10 2.2.1 Meteorology and boundary concentrations

11 In the present study we force MATCH with three-dimensional meteorology from the
12 numerical weather forecast model HIRLAM. Within the EURO4M-project
13 (<http://www.euro4m.eu>) HIRLAM was run as forecasts from 6-hourly analyses, composed of
14 variational upper air analyses in 3 dimensions and optimal interpolation surface analyses.
15 Lateral and lower (sea surface temperature and sea ice) boundaries were taken from ERA-
16 Interim (Dee et al., 2011). Full three-dimensional model states needed to run MATCH are
17 available from 1979 through February 2014. Under EURO4M, HIRLAM was running on a
18 domain covering Europe and Northern Africa with 22 km grid point spacing and 60 vertical
19 layers from the surface to 10 hPa.

20 Although the present study focuses on Sweden it is necessary to realistically describe the
21 fluxes of O₃ from continental Europe and further afield. Hemispheric concentrations of all
22 species are similar to the ones used by Andersson et al. (2007) for the modelled year 2000. As
23 in Andersson et al. (2007), boundary values representative for the lateral and top boundaries
24 of relevant species are interpolated spatially with a monthly temporal resolution. Boundary
25 concentrations of O₃, oxidized nitrogen and methane are scaled to mimic observed changes in
26 the hemispheric background during the period 1990 through 2013 (cf. Fig. 2a). The same
27 factor is used for all months of the respective year, although most species also undergo a
28 seasonal cycle in the boundary concentrations used by MATCH (see supplement Fig. S1).

29



1 2.2.2 Emissions

2 The version of MATCH utilized in this study needs anthropogenic emissions of sulfur (SO₂
3 and sulfate), nitrogen oxides (NO and NO₂), carbon monoxide (CO), non-methane volatile
4 organic compounds (NMVOCs), and ammonia (NH₃). The model uses annually accumulated
5 values for each species, which are distributed with different temporal or vertical profiles
6 based on species and sectors.

7 For countries outside Sweden (as well as international shipping) we utilize the gridded (50 km
8 × 50 km) annual data available at EMEP's web-page (<http://www.emep.int>; downloaded 23
9 June, 2015). All emission data were split into congruent 5 km × 5 km cells where we replaced
10 the coarse-resolution data over Sweden with the original emission data from SMED (Svensk
11 miljöemissionsdata; <http://www.smed.se>; 1 km × 1 km converted to 5 km × 5 km cells in
12 EMEP's geometry). National totals from SMED are very similar to the national totals
13 available in the EMEP database, but our methodology enables higher resolution emission data
14 over Sweden. The gridded 5 km × 5 km emission data were interpolated to MATCH's 44 km
15 resolution domain during the simulations.

16 Both the total domain and Swedish anthropogenic O₃ precursor emissions decrease strongly
17 over the period 1990-2013 (cf. Fig. 2b). The total domain anthropogenic precursor emissions
18 decrease on average¹ by 1.8 % yr⁻¹, 2.4 % yr⁻¹, 2.6 % yr⁻¹ during 1990-2013 for NO_x,
19 NMVOC and CO respectively, whereas biogenic isoprene emissions (calculated online by
20 MATCH) increase by 0.8 % yr⁻¹ according to our simulations. The Swedish emissions
21 decrease by similar amounts (2.4 % yr⁻¹, 2.1 % yr⁻¹ and 2.9 % yr⁻¹). The Swedish contribution
22 to the total domain emissions is 1.0 % for NO_x and 1.7 % for NMVOC and CO on the
23 average, with a slight decrease in the relative Swedish contribution over the period for NO_x
24 (0.01% yr⁻¹), and a slight increase for NMVOC and CO (0.01 % yr⁻¹ and 0.003 % yr⁻¹
25 respectively). We assume that there is no trend in the temporal intra-annual variation of the
26 emissions.

27

¹ The trend is calculated by linear regression over the period 1990-2013 and related to the 1990 emission level.



1 2.3 Measurements

2 Figures 3 and 4 summarize the observations of hourly O₃ concentrations used in the
3 variational analysis and the corresponding hourly data coverage per year in the period 1990-
4 2013. These measurements represent the regional background in Sweden and Norway. The
5 sites included are all instrumentation sites, where O₃ is measured continuously and reported
6 with hourly temporal resolution. The data assimilation is conducted on hourly resolution,
7 which means that measurements with a coarser time resolution, such as diffusive samplers,
8 are not included in the variational technique. Two measurement data sets were compiled (see
9 Table 1):

- 10 • The first includes data from all available instrumentation sites in Sweden, and a
11 selection in Norway based on data availability, quality and location. These are all the
12 red and blue sites in Figs. 3 and 4 also including years where the data capture is lower
13 than 80 %. The reanalysis based on these measurement data is called ALL.
- 14 • The second data set includes data from instrumentation sites for which the data
15 coverage exceeds 80 % for at least 23 out of the 24 years. These are the red sites in
16 Figs. 3 and 4. The reanalysis based on these measurement data is called LONGTERM.
17 Råö is seen as the replacement for the site Rörvik, and therefore these sites form a
18 pair, which is included in this data set. Birkenes I was replaced by Birkenes II in 2009,
19 and the two sites were run in parallel for a few years. We choose to include Birkenes
20 II from 2010 and onwards. The reason for the change of site location is that Birkenes I
21 was influenced by local effects, such as night-time inversions (personal
22 communication with Sverre Solberg, NILU). The inclusion of these two sites could
23 introduce an artificial trend in the reanalysis, but since it is outside the main focus area
24 (Sweden) and mainly during night we choose to include the site in the LONGTERM
25 reanalysis.

26 The two measurement data sets are input to two otherwise similar data assimilations. The
27 ALL-reanalysis is our best estimate of gridded near-surface O₃ over Sweden for a given time.
28 The LONGTERM-reanalysis is used for trend and statistical analyses. This is because
29 changes in the number of sites and data coverage in the ALL data set can introduce artificial
30 trends due to model biases being corrected by observations included in the later part of the
31 period but not in the first. We return to whether these reanalyses differ in Sect. 3.1.



1

2 **2.4 Data assimilation**

3 The spatial analysis problem can be formulated as how to best distribute observational
4 information at a discreet number of locations to a spatially consistent field. We have adopted
5 the 2dvar approach, which includes a modelled background field (from a CTM simulation,
6 “first guess”) combined with available in situ observations (Robertson and Kahnert, 2007), as
7 indicated in Fig. 1. With this method the error estimates of both the background field and the
8 observations play a central role. The observational errors are assumed independent and
9 uncorrelated, while the background errors have spatial correlations that form a background
10 error matrix. The solution is found by the best combination of the background field and
11 observations given their respective error estimates. This can be described as a variational
12 problem, defined by a cost function,

$$13 \quad J(x) = 0.5 [x - x^b]^T \mathbf{B}^{-1} [x - x^b] + 0.5 [y - \mathbf{H}(x)]^T \mathbf{O}^{-1} [y - \mathbf{H}(x)]$$

14 where x is the state to be found (the reanalysis), x^b the background state (our “first guess”), y
15 the vector of observations, \mathbf{H} is the observation operator, and \mathbf{B} and \mathbf{O} are the error
16 covariance matrices of the background field and the observations, respectively. In order to
17 find the optimal solution the cost function is stepwise minimized by a variational method,
18 starting with $x = x^b$, and ending with the state x , which represents the optimal balance between
19 the two terms. During the process the co-variances in the \mathbf{B} matrix acts to extrapolate the
20 observational information in space.

21 We restrict our study to reanalyze near-surface O_3 on the regional background scale, which
22 means we only include regional background measurement sites. We also restrict our study to
23 2dvar, rather than using higher dimensional variational analysis. The background covariance
24 matrix is modelled in a simplified fashion with a constant background error, 20 times larger
25 than the observation error, and Gaussian spatial correlations with a length scale of 1000 km.
26 This implies a strong weight towards the observations and assuming a rather large horizontal
27 influence of the observations, which is related to the rather sparse network of regional
28 background observations and the relatively small emissions of O_3 precursors in Sweden
29 resulting in weak horizontal gradients of near-surface O_3 on the regional background scale.

30 The data assimilation was conducted on a 22 km resolution grid with hourly temporal
31 resolution, combining the modelled “first guess” for near-surface O_3 (the MATCH base case



1 scenario, MFG in Table 1) and regional background measurements. Two 24-year reanalyses
2 were formed, using the two sets of hourly measurement described in Sect. 2.3 (ALL and
3 LONGTERM in Table 1). If an included measurement site was lacking an observation for a
4 specific hour, the site was excluded from the data assimilation for that specific hour.

5 The resulting spatially resolved hourly O₃ data are used to form annual and seasonal statistical
6 metrics for O₃, such as the mean value and the maximum 1-hour mean value, and annual
7 policy and impact related metrics (cf. Fig. 1). We analyze these annual and seasonal data for
8 the 1990-2013 mean, trend and extreme values in Sect. 3.2 (annual/seasonal mean and
9 maximum) and Sect. 3.4 (health and vegetation impact metrics).

10

11 **2.5 Understanding the trends**

12 We include also a quantification of the causes to the trend in near-surface O₃ concentration.
13 For this investigation we conduct model simulations with MATCH, *excluding data*
14 *assimilation*. We investigate the respective contributions to the modelled total trend due to

15 A. Change in emissions, which is separated between

16 o Swedish anthropogenic emissions (Se emis)

17 o European (full domain) non-Swedish anthropogenic emissions (Eur emis)

18 B. Change in lateral and upper boundaries (bound)

19 C. Change in meteorology, including online modelled biogenic isoprene emissions
20 (meteo)

21 Four sensitivity simulations are conducted; in which each of the four listed processes are kept
22 constant at the level in 2011. The respective contributions to the trend are formed by
23 subtracting the MFG with the corresponding sensitivity simulation. All model simulations and
24 scenarios are described in Table 1a. The method of forming the contributions from these
25 simulations is shown in Table 1b.

26 There are two critical points in the investigation of the causes of the trend: First, this
27 quantification methodology assumes linearity, whereas the sum of contributions (SUM) is not
28 necessarily equal to the trend in the MFG simulation. If they are not equal, this means that the
29 simulation is non-additive. This could occur when changes to mixtures of complex chemistry,



1 weather situations and emissions take place. For this reason we compare the sum of the trend
2 in the estimated contributions to the MFG trend. Second, we quantify the contributions to the
3 trend in the MFG simulation, which may differ from the reanalyzed trend. Thus we will
4 compare the reanalyzed trend and the base case trend to make sure the base case simulation
5 does not deviate too strongly from the reanalysis results. If the deviation is too large, i.e. the
6 modelled trend is far from the observed, this means that it is non-representative. Such
7 discrepancies could arise from over-sensitivity in MATCH to one process and insensitivity to
8 another, compared to the real world, or imperfections/artificial trends in the input data such as
9 erroneously estimated emissions or erroneous assumptions on the trend in hemispheric
10 background concentrations. If either is true (non-representative or non-additive) for the trend
11 in a specific metric, such as the trend in the January mean, then our method cannot be used to
12 explain that specific trend.

13

14 **2.6 Evaluation**

15 We evaluate two aspects of the reanalysis. The first is an independent evaluation for a single
16 year with focus on the data assimilation method. The second is an evaluation of the simulated
17 near-surface O₃ concentration trend over the period and our ability to explain the causes of the
18 trend.

19 For an independent evaluation of data assimilation method we conduct a cross validation at
20 the included Swedish measurement sites. With this method we exclude one measurement site
21 at a time from the data assimilation, and use the analysis results from the excluded location in
22 the evaluation of all sites. This means we conduct one such 2dvar simulation for each
23 considered measurement site. Due to the large amount of computation involved we evaluate
24 one year only by this method. We choose the year 2013, which is when the data coverage is
25 the largest. This means that we have the opportunity also to investigate whether we see any
26 difference in performance between the reanalysis with the larger number of measurement sites
27 (ALL) and the long-term reanalysis (LONGTERM). The evaluation metrics used here are
28 mean value (mean), standard deviation (σ), model mean bias normalized by the observed
29 mean (%bias), Pearson correlation coefficient (r) and the root mean square error (RMSE), see
30 Supplement Sect. S1.



1 For the evaluation of the long-term trend we focus on the two critical points raised in the
2 previous section: 1/ the additivity of the trend in the contributions as compared to the trend in
3 O₃ concentration from the MFG simulation, and 2/ whether the MFG trend is representative
4 of the O₃ concentration trend in the LONGTERM reanalysis results. We focus this
5 investigation on 11 different percentiles of hourly mean O₃ concentrations, for an estimate of
6 the scores at different concentration levels. We focus specifically on averages over the three
7 Swedish regions North, Central and South (cf. Fig. 3), to investigate whether there is any
8 variation in performance in Sweden. The comparisons are presented as scatterplots in Fig. 5
9 and compared to the 1:1 line, factor 2 line and equal sign quadrants.

10 Additional evaluation and comparisons of the temporal variation over the whole period is
11 included in the Supplements for the two reanalyzes LONGTERM and ALL, the MATCH
12 simulation MFG and observed annual mean (see Supplement Sect. S2 and Figs. S2-S4 and
13 Table S1).

14

15 **3 Results**

16 **3.1 The performance of the model simulations and reanalyzes**

17 Before turning to the evaluation results, we investigate whether the two ozone reanalyzes
18 differ. We do this by comparing time series of annual O₃ metrics for the two data sets. The
19 investigation is presented in the Supplements and shows deviations in the latter years as the
20 number of sites in the ALL data set increases beyond the sites included in the LONGTERM
21 data set (see Supplement Sect. S3 and Figs. S2-S4). The deviation in annual mean near-
22 surface O₃ concentration is larger than for annual maximum 1 hour mean given that many of
23 the newer sites are sensitive to night-time inversions. Due to the visible deviation in results,
24 we use the LONGTERM for the trend and statistical analyzes in the paper, whereas both are
25 used for the evaluation of the 2dvar-method in this section. Both are included in the method
26 evaluation because the evaluation scores may be dependent on the density and specific
27 locations of the measurement sites. The ALL data set is to be used as a best estimate of
28 geographically resolved near-surface O₃ concentrations for Sweden for a subset period within
29 the full period 1990-2013.

30 In Table 2 we show the evaluation statistics from the validation of hourly near-surface O₃ in
31 2013. The near-surface O₃ concentrations from the MFG simulation compare well with



1 observations, and the 2dvar-technique leads to improvements. The spatially averaged
2 correlation coefficient of hourly near-surface O₃ concentrations (see Supplement Sect S1
3 increases from 0.67 when comparing the MFG O₃ concentrations to observations, to 0.76
4 when comparing the ALL reanalysis independently to observations through a cross validation
5 (Table 2). The %bias decreases from 1.4 to -0.3 and the RMSE is also improved in the
6 independent evaluation of the ALL reanalysis. Similar improvements are also obtained when
7 using fewer measurements (LONGTERM, Table 2), showing that the method is stable with
8 the number of measurement sites. The cross validation spatial error (RMSE) is however
9 larger than that obtained when evaluating the MFG simulation against independent
10 observations, where the cross validation results indicates that the 2dvar reduces the quality of
11 the annual mean spatial variation in 2013. The lowest annual means in 2013 (Supplement
12 Table S2) are found in the sites Rödeby, Aspvreten, Östad, Norr Malma and Asa, where the
13 annual means are below 30 ppb(v). The highest annual means are found in Esrange, Norra
14 Kvill, Råö and Vavihill. This is likely caused by strong night-time inversions in the sites with
15 lower annual means. These night-time inversions depend to a large extent on local
16 topography, and are not uncommon in inland sites positioned at a low altitude in the local
17 landscape compared to the average of the surrounding area. This variation occurs at a higher
18 resolution than is captured by the MFG simulation (44km resolution). Simultaneously the
19 correction of the model by the data assimilation based on the differences between the model
20 and the measurements, results in readjustments of the model results for the surrounding area
21 and specifically for other sites not affected by night-time inversions. This is illustrated in the
22 Supplements (Fig. S5). Overall, the independent cross validation shows that the 2dvar method
23 improves the performance of the modelled hourly mean O₃ compared to the MFG simulation.
24 This is true not only in the measurement sites, but also elsewhere, with exception for the
25 spatial variation in annual mean.

26 In Fig. 5 we compare trends in annual near-surface O₃ percentiles over the period 1990-2013
27 for the MFG simulation, the LONGTERM reanalysis and the sum of contributions.
28 Investigating the additivity of the four contributions (bound, meteo, Se emis and Eur emis),
29 we compare the O₃ concentration trends in the MFG simulation to the trend in the sum of the
30 contributions (SUM, Fig. 5a). Almost all values fall close to the 1:1 line. Only a few of the
31 very weakest O₃ trends fall outside the factor 2 lines. Thus, the contribution experiment can
32 be used to explain the MFG O₃ trend. Comparing the LONGTERM and MFG trends in near-
33 surface O₃ (Fig. 5b), the values are within a factor of 2 for most percentiles and regions. There



1 is a general tendency for the positive MFG trends to be stronger than the reanalyzed trend
2 (LONGTERM). The largest deviations in the O₃ trends are in the North and the relationship
3 between these two is not as linear as in the other two regions. Most of these trends are
4 however not significant. This demonstrates the added value of the measurement model fusion,
5 where errors in the modelled trend are corrected by the analysis. The deviations are small
6 enough to conclude that in most cases the MFG is representative, showing that the MATCH
7 model can be used to understand the trends in the LONGTERM data set.

8 In conclusion we have shown that the MFG performs well for hourly near-surface O₃
9 concentration and the 2dvar analysis improves the performance to almost perfect
10 correspondence to the measurements in the measurement locations, and improved
11 performance elsewhere (cf. the cross-validation), with the exception of the spatial variation.
12 There is an added value of a reanalysis when investigating the trend of near-surface O₃
13 concentrations. The MATCH model can be used to investigate the causes to the reanalyzed O₃
14 trend. In the North the trends in the reanalyzed and the MFG O₃ concentration deviates by
15 more than a factor of 2 for some percentiles. We will focus on this deviation more in the final
16 discussion (Sect. 4).

17

18 **3.2 Reanalyzed near-surface ozone in Sweden 1990-2013**

19 The mean 1990-2013 seasonal variations in monthly mean and monthly maximum of 1h mean
20 near-surface O₃ are presented in Fig. 6, averaged over the three regions: North, Central and
21 South (as defined in Fig. 3). Spatially resolved statistics for annual mean and annual
22 maximum of 1h mean near-surface O₃ are provided in Fig. 7. Time series of annual
23 percentiles averaged over the three regions are shown in Fig. 8.

24 **3.2.1 1990-2013 period statistics**

25 The near-surface O₃ in Sweden exhibits a seasonal variation, which peaks during spring (Fig.
26 6). In the North the seasonal maximum concentration occurs in April, whereas it occurs later,
27 in May, in the regions further south. The earlier peak in the North, as compared to the South,
28 was also shown by Klingberg et al. (2009) for in situ observations. In the North, the seasonal
29 peak in monthly mean O₃ concentration is higher than the corresponding seasonal peaks in the
30 other two regions, and this is a feature throughout the whole winter half-year: the monthly



1 mean O₃ concentrations are higher in the North than the more southerly regions during Oct-
2 April. During the summer, the monthly means are higher in the South than in the other two
3 regions. This leads to a 24-year period mean value (Fig. 7) that is highest in the northerly
4 mountains and lowest in central Sweden. This pattern is also supported by Klingberg et al.
5 (2009) based purely on observations, but including a larger number of observation sites
6 through the inclusion of passive diffusion samplers.

7 For the period mean seasonal variation in monthly maximum 1h mean near-surface O₃ (Fig.
8 6b) there is a similar seasonal peak in April-May, but there is also a secondary peak during
9 summer (in August). The further south the higher is the monthly maximum 1h mean near-
10 surface O₃ during March-October. This applies to both the primary and the secondary
11 seasonal peaks in monthly maximum. The 24-year period mean of the annual maximum of 1h
12 mean near-surface O₃ (Fig. 7) is lower in central Sweden than in the South and the North, and
13 it is highest in the South.

14 The lower period mean of the near-surface O₃ in the South than in the North is possibly
15 caused by night-time inversions at some of the southerly sites, and also therefore the reason
16 for the opposite gradient for the annual maximum 1h mean as compared to the annual mean.
17 The difference in spatial pattern between the south, central and northern parts of Sweden is
18 why we choose the three regions defined in Fig. 3. The period maximum of the annual means
19 and period maximum 1h mean near-surface O₃ concentrations have similar spatial variation as
20 the period means (Fig. 7). The overall 24-year maximum 1h mean near-surface O₃ reaches
21 above 240 µg m⁻³ in isolated parts of the South, and is generally above 180 µg m⁻³ in the south
22 and 130 µg m⁻³ in the central and northern part of Sweden.

23 3.2.2 Trend over the period

24 Seasonal variations are also present in the trend of both monthly mean and monthly maximum
25 1h mean near-surface O₃ concentrations (Fig. 6). Monthly means increase strongly during
26 winter and spring (approx. Nov-April), and decrease moderately (North) or strongly (Central
27 and South) during summer (May-Aug). The trends in monthly maximum 1h mean follow a
28 similar pattern. Generally, the rate of change is stronger or at the same level in the Central and
29 South as compared to the North. The strongest decrease is in the August maximum 1h mean
30 in the South and Central, and the strongest increase is in the March monthly mean. The day of
31 the year when the annual maximum 1h mean near-surface O₃ occurs shifts to earlier in the



1 year in the later part of the period, although there is large inter-annual variation, which is
2 stronger in the South than in the North (Supplements Fig. S6).

3 The annual mean near-surface O₃ (Fig. 7d,e) increases almost everywhere in Sweden over the
4 time period. The trend is however only significant in restricted parts of Central and South
5 regions, due to considerable inter-annual variation in the areas with the highest trend. The
6 annual maximum 1h mean near-surface O₃ (Fig. 7i,j) is significantly decreasing in South and
7 Central regions, whereas the change in the North is a mixture of increase and decrease, and it
8 is without significance in most areas. The decrease in the South and Central annual maximum
9 1h mean is a result of the strong decrease in the summer-time O₃ maximum; in the beginning
10 of the 24-year period, the southern summer-time maximum is more often the annual peak
11 rather than the spring-time maximum, whereas the summer-time maximum is more often
12 secondary to the annual maximum in the end of the period. The annual maximum 1h mean is
13 shifted to earlier in the year (Supplements Fig. S6). In a study of four rural European sites and
14 one in western United States, Parrish et al. (2013) showed that not only are springtime O₃
15 concentrations larger in recent years than in earlier decades, but also that the seasonal
16 maximum now also occurs earlier, as in our results for Sweden. This change in seasonal cycle
17 is also supported by the work by Cooper et al. (2014). The change in the annual maximum 1h
18 mean near-surface O₃ from summer-time peak to spring-time peak means that more than one
19 process can be the cause of the change (increasing spring-time and decreasing summer-time).

20 We proceed by investigating the trend in annual percentiles of hourly near-surface O₃
21 concentration, averaged² over the three Swedish regions (cf. Fig. 3). The temporal evolution
22 of 11 percentile levels from the 0th (annual minimum 1h mean) to the 100th (annual maximum
23 1h mean) are shown in Fig. 8, and the corresponding trends with indication of significance
24 levels are recaptured in the Supplements (Table S3). In all three regions the low and medium
25 percentiles are increasing, while the highest percentiles are decreasing from 1990 until 2013.
26 This was also shown by Simpson et al. (2014) based on observations for northern Europe and
27 based on observations for Europe, US and East Asia by Lefohn et al. (2017). Further, using
28 hourly O₃ observations, Karlsson et al. (2017) showed that reduced concentrations were

² The percentile is calculated per grid square for all hours in each year, then regional mean annual percentiles are calculated and finally the trend is calculated based on these averaged percentiles.



1 restricted to the highest O₃ concentrations during summer daytime, while the increase in low
2 and mid-range concentrations occurred during wintertime at both day and night.

3 In Central and South regions the decrease in the highest near-surface O₃ percentiles are
4 stronger than in the North, and significant and this decrease is evident throughout the
5 maximum 10% percentile range (although the change is not significant for the 90th and 95th
6 percentile levels; cf. Fig 3). This change is mainly caused by decreased high values during the
7 summer-time. In the North, only the annual maximum 1h mean is decreasing and the inter-
8 annual variability is stronger than the rate of change, indicated by the lack of significance for
9 this percentile. The medium and low percentile increase in the North is moderate, but
10 significant, for most percentiles up to the 95th, with very similar rates of change. In the
11 Central and South the change in the low percentiles is highly significant and stronger than in
12 the North. This is an indication that the increase in low near-surface O₃ concentrations cannot
13 only be explained by increasing background. As a result of the decrease of high and increases
14 of low percentiles, there has been a narrowing of the range of the near-surface O₃
15 concentrations over the period. This was also observed in the US by Simon et al. (2015) for
16 1998-2013, studying urban and regional background measurements across the US. They
17 interpret this as a response to the substantial decrease in O₃ precursor emissions in the US
18 over the time period. Decreased primary NO emissions results in decreased O₃ titration close
19 to combustion sources, but also reduces local O₃ further away from the emissions sources
20 under weather states favorable for O₃ formation. In the next section we investigate the impact
21 of Swedish and European emission decrease over the period, and relate this to the impact of
22 change in the chemical composition of the hemispheric background and meteorological
23 variations.

24

25 **3.3 Attribution of the change in near-surface ozone**

26 In this section we quantify the contributions of physical processes to the modelled trend of
27 near-surface O₃ concentration in Sweden during the period 1990-2013. We investigate the
28 impact of the trend in lateral and upper boundaries, meteorological variations and Swedish
29 and European (non-Swedish, full domain) anthropogenic emission change. In Figs. 9 and 10
30 the contributions to the trend in seasonal variations and percentiles are quantified for the
31 North and South regions.



1 We start our attribution by analyzing the impact of changing hemispheric background levels
2 of relevant chemical species (“bound” bars in Figs. 9 and 10). These show an increase in
3 monthly mean and maximum 1h mean throughout the year and for all percentiles, mainly as a
4 result of our assumption of an increasing O₃ concentration trend in the lateral and upper
5 boundaries during the 1990s and constant boundary conditions for O₃ during the rest of the
6 period. There is a seasonal variation in the trend of the boundary contribution, with a
7 minimum during summer. This variation is likely a result of an O₃ destruction process that is
8 stronger during summer than winter, such as dry deposition to vegetation and photolysis of
9 ozone. The seasonal variation in the contribution to the trend from the boundary impacts both
10 monthly mean and maximum 1h mean. Our representation of the trend in the concentration of
11 species at the model domain boundary is climatological. The climatological upper boundary
12 means that the inter-annual variations in near-surface O₃ are likely underestimated in remote
13 locations. The impact on inter-annual variations may be largest at high altitudes or far away
14 from the major anthropogenic sources. Hess and Zbinden (2013) showed the importance of
15 the stratospheric contribution to the inter-annual variation at Mace Head and Jungfraujoch; it
16 is possibly also important in the north of Sweden, especially in the mountainous areas. Such
17 variation is not captured by the boundary settings, but it is indirectly included in the
18 reanalyzes data sets through the variation in the measurements included in the data
19 assimilation. As a consequence, the MFG and “bound” simulations underestimate the inter-
20 annual variability as compared to observations and the reanalysis (cf. Table 2), and this could
21 also affect the “bound” trend.

22 The impact of meteorological low-frequency variations (“meteo”) during the 24 years is also
23 an important factor, but more difficult to interpret. The meteorological variation acts to cause
24 a positive trend in near-surface O₃ concentration for most monthly means and maxima, as
25 well as for most percentiles. The meteorological influence on the trend is as large as the
26 impact of the change in boundary, for most percentile levels in the South, while it is weaker
27 for most percentile levels in the North.

28 During the period 1990-2013 both European (full domain, non-Swedish) and Swedish
29 emissions have decreased strongly. There is a strong seasonality in the impact of the
30 decreasing European emissions, and the contribution to the trend of the Swedish emissions
31 follows the same pattern but with smaller magnitude (cf. Fig. 9, “Eur emis” and “Se emis”
32 respectively). During summer the decreasing emissions have acted to lower both the monthly



1 mean and maximum 1h mean. During winter the trend in monthly maximum 1h mean is
2 unaffected by the change in emissions, indicating that the highest near-surface O₃
3 concentrations during winter are due to other sources than local O₃ production. Emission
4 decreases have acted to cause increases in monthly mean near-surface O₃ concentrations in
5 the winter, due to reduced O₃ destruction by primary NO emission. Trends in percentiles (Fig.
6 10), show that the emission decrease has caused decreases to percentiles higher than the 50th
7 level, and increases below. The impact is stronger in the South than in the North, which is
8 expected due to the South being closer to the European continent. The contribution of the
9 trend in emissions is often stronger than the changing boundary, e.g. in the South for most
10 percentiles and for monthly maximum 1h mean during the summer half-year in both regions.
11 Thus, the observed increase in low and medium near-surface O₃ levels is caused by a mixture
12 of both changes to the hemispheric background levels and emission reductions of O₃
13 precursors, while the decrease in the high percentile levels is mainly caused by emission
14 decrease.

15

16 3.4 Implications for health and vegetation impacts

17 For the protection of vegetation, the target value by EU (EU directive 2008/50/EC) states that
18 the 5-year mean AOT40 (near-surface O₃ concentration above 40 ppb(v) accumulated over
19 May-July; AOT40c) must not exceed 9 ppm(v) h, and as a long-term goal AOT40c must not
20 exceed 3 ppm(v) h during a calendar year. For protection of human health the target value by
21 EU (EU directive 2008/50/EC) states that the daily maximum running 8 hour mean near-
22 surface O₃ concentration must not exceed 120 µg m⁻³ more than 25 days per year as a 3-year
23 mean, and as a long-term goal the daily maximum of 8h mean near-surface O₃ concentration
24 must not exceed 120 µg m⁻³ at all. Sweden has formulated 16 environmental quality
25 objectives, including clean air, alongside specifications to help reach these objectives. The
26 following specifications are currently valid for near-surface O₃ concentration in Sweden (NV,
27 2015): the hourly mean must not exceed 80 µg m⁻³, the daily maximum 8h mean must not
28 exceed 70 µg m⁻³ and AOT40f (O₃ concentration above 40 ppb(v) accumulated over April-
29 September) must not exceed 5 ppm(v) h. In Table 3 we present the linear trends in our
30 reanalysis data set for these metrics, and have collected geographically resolved statistics,
31 such as the period mean, maximum and linear trend in the Supplements (Figs. S7-S11).



1 The narrowing of the O₃ concentration range, especially through increasing lower percentiles,
2 can impact human and vegetation exposure to O₃. The effect metrics based on accumulation
3 of values above a threshold (AOT40c; AOT40f; SOMO35, Sum of Ozone Means³ Over 35
4 ppb(v)) and the number of days with daily maximum of 8h mean near-surface O₃
5 concentration exceeding 120 µg m⁻³ have been decreasing over the period in the South and
6 Central regions, as have the highest values in the year. This is in accordance with the decrease
7 in the highest percentiles in these regions (cf. Supplements Table S3). Conversely, the metrics
8 with lower threshold values increase, such as the number of hours exceeding 80 µg m⁻³ and
9 the number of days with daily maximum 8h mean near-surface O₃ concentration exceeding 70
10 µg m⁻³. This increase is significant in the North, whilst it is not significant in the South and
11 Central. This agrees with the change in medium and low percentiles. A continued increase in
12 low values would cause a continued increase in these metrics, and would eventually reverse
13 the decreasing trend to an increase. This is valid specifically for those metrics with
14 accumulation of values or higher thresholds, such as SOMO35 and AOT40c.

15 The highest near-surface O₃ concentrations, associated with short-term (acute) health impacts,
16 show a clear and significant decrease in the South (where the highest values occur), leading to
17 an improvement in health impacts. For long-term health effects, there is no established
18 threshold below which there are no adverse effects, even if SOMO35 often is used. The
19 increase in low values (and e.g. the annual mean) has negative impacts on health, although
20 SOMO35 is decreasing in the South and Central Sweden. This increase is also of concern
21 given that policy choices will cause further reductions in local NO emissions – which are
22 highly correlated to where people reside – thus increasing the sensitivity of O₃ to the
23 background and hemispheric background level. Despite this, the solution is not to reverse
24 policies that reduce local NO production, given that this would negatively impact both the
25 highest values and the hemispheric background. A solution must therefore be sought via
26 international policy regulations.

27

³ For SOMO35 the Mean is defined as the daily maximum of running 8h mean near-surface O₃ concentrations and the accumulation is over a year unless otherwise is stated.



1 **4 Discussion**

2 This work improves upon previous studies by investigating the trends in near-surface O₃
3 concentration via a combination of both observed and modelled knowledge. The respective
4 advantages of modeling (geographical and temporal coverage) and observations (the most
5 reliable O₃ concentration estimate at a discreet point) can be exploited through data
6 assimilation to reach a greater understanding of the atmospheric state, and the model can
7 further be used as a tool to explain what is described.

8 Our results should, however, also be viewed in the context of their limitations. The model
9 simulations have a relatively coarse horizontal resolution, meaning that processes that are
10 more local in origin are not captured by the model – these include the role of local topography
11 or coastal climate for the night-time boundary layer stability (Klingberg et al., 2011), or local
12 emission sources. As a result, the data assimilation scheme will spread such features to parts
13 of the model where they are not valid. Some of the southerly sites in the data assimilation are
14 known to experience night-time inversions and the reanalysis will thus be affected by this. We
15 choose however not to exclude these data from the data assimilation, on the basis that this is
16 restricted to occasional events during night-time. An improvement in the spatial resolution of
17 the model would improve the spatial representation of the analysis, since the difference
18 between observation and model has the potential to decrease at these observation sites.

19 As with all modeling studies, the model cannot perform better than the quality of the forcing
20 input data. Knowledge of emissions in the beginning of the 24-year period is less
21 comprehensive than at the end, which could introduce artificial trends to the MFG. The trends
22 in lateral and boundary conditions are taken from the work by Engardt et al. (2017) and are
23 based on observed trends at the lateral boundaries of Europe. The upper boundaries are
24 especially poorly represented, and as a consequence so is the stratospheric contribution to the
25 inter-annual variation and trend. The data assimilation reduces the impact of errors in the
26 lateral and upper model boundaries. However, the reanalysis may still be affected in regions
27 with sparse measurement coverage. This can affect the attribution to the trend. In this study
28 the MFG simulation captures the observed (reanalyzed) trend reasonably well, but there is a
29 discrepancy between the reanalysis and MFG trend for most percentile levels in North
30 Sweden. To investigate this in more detail, we have compared the error in trend by percentile
31 (the difference between the trends in MFG and LONGTERM) to the trend caused by the four
32 contributions (bound, meteo, Se emis and Eur emis). The resulting figure is included in the



1 Supplements (Fig. S12). There is a 1:1 relation between the impact of the trend in the
2 European emissions and the deviation between the MFG and the LONGTERM trends. This
3 could be caused by overestimation of the European emissions trend. A similar tendency is
4 seen for the Swedish emission contribution in the Central and South regions. This calls for
5 emission inventories to be improved in order to make sure the trend in ozone precursor
6 emissions is correct. Another reason for this could be too strong model sensitivity to the
7 European emission trend in the North. If this was true, it would have implications for
8 sensitivity studies that consider the future development of near-surface O₃. In studies relating
9 the impacts of future climate change to future anthropogenic precursor emission change, a
10 robust conclusion for most models is that the impact on near-surface O₃ concentration of
11 future precursor emissions is much stronger than the impact of climate change (e.g. Engardt et
12 al., 2009, Langner et al, 2012; Watson et al., 2016). If models are too sensitive to trends in
13 emissions in remote areas, compared to other processes, such a conclusion might change.
14 Parrish et al. (2014) also compared observed and modelled trends and found that the three
15 chemistry-climate models studied failed to reproduce the observed trends – the modelled O₃
16 concentration trend was approximately parallel to the estimated trend in anthropogenic
17 precursor emissions of NO_x, whilst observed O₃ concentration changes increased more rapidly
18 than these emission estimates. This implies that there is a lack of knowledge relating to
19 controls of concentrations of tropospheric O₃. Whether it is the trend in ozone precursor
20 emissions or the model sensitivity to emissions that need improving is left for future studies.

21 Finally, we conducted a trend analysis of the reanalyzed near-surface O₃ using linear
22 regression. We have chosen to present the trend in the LONGTERM data set in all analyzes,
23 regardless of whether it is statistically significant or not. We stress that a trend contains valid
24 information even where it is not statistically significant – and it will become significant if the
25 change and variability remains the same over time. We also recognize that there are other
26 methods of investigating the statistical behavior of the data set, and therefore welcome further
27 use of the data, which may be accessed upon request from the corresponding author.

28

29 5 Conclusions

- 30 • We have constructed two hourly reanalyzes of near-surface O₃ for Sweden for the
31 period 1990-2013: one time-consistent reanalysis and one using all available hourly



1 measurements. Both data sets are available upon request from the corresponding
2 author.

3 • We have evaluated the performance of the reanalyzed near-surface O₃ and mainly
4 found improved performance compared to the MATCH model.

5 • Our results show:

6 ○ High near-surface O₃ concentrations in Sweden are decreasing and low O₃
7 concentrations are increasing.

8 ○ Health and vegetation impacts due to high near-surface O₃ concentrations
9 (quantified by policy related threshold metrics) have decreased in Sweden as a
10 result of the decrease in the highest ozone values.

11 ○ Decreasing emissions in Europe have led to decreasing summer-time near-
12 surface O₃ concentrations, as well as a decrease of the highest concentrations.

13 ○ The rising low concentrations of near-surface O₃ in Sweden are caused by a
14 combination of rising hemispheric background O₃ concentrations,
15 meteorological variations and O₃ response to European O₃ precursor emission
16 regulation.

17 ○ There is a discrepancy between modelled and observed (reanalyzed) O₃ trends
18 in northern Sweden. This could be caused by erroneous trends in the historical
19 anthropogenic ozone precursor emissions used here or that our model is too
20 sensitive to changes in emissions. If the latter is true, it implies that the
21 evolution of future precursor emissions may have a smaller impact on future
22 near-surface O₃ concentrations than shown by earlier studies.

23

24 **Acknowledgements**

25 This project was funded by the Swedish Environmental Protection Agency (EPA), through
26 funding directly to the reanalysis (contract no. 2251-14-016) and through the research
27 program Swedish Clean Air and Climate (SCAC) and NordForsk through the research
28 programme Nordic WelfAir (grant no. 75007). The annual mapping with the MATCH
29 Sweden system is funded by the Swedish EPA.



- 1 Thank you to Sverre Solberg (NILU, Norway) for all help, especially with the selection of
- 2 Norwegian observation sites.
- 3



1 **References**

- 2 Akimoto, H.: Global air quality and pollution, *Science*, 302, 1716-1719,
3 doi:10.1126/science.1092666, 2003.
- 4 Alpfjord, H. and Andersson, C.: Nationell miljöövervakning med MATCH Sverige-systemet
5 – ny metodik, utvärdering och resultat för åren 2012-2013, Swedish Meteorological and
6 Hydrological Institute, Norrköping, Sweden, SMHI report nr 2015-7 (in Swedish), 45pp,
7 available at internet URL: <http://www.smhi.se/klimatdata/miljo/atmosfarskemi> (last access
8 March, 2017), 2015.
- 9 Andersson, C., Langner, J., and Bergström, R.: Interannual variation and trends in air
10 pollution over Europe due to climate variability during 1958–2001 simulated with a regional
11 CTM coupled to the ERA40 reanalysis, *Tellus B* 59, 77-98, doi: 10.1111/j.1600-
12 0889.2006.00196.x, 2007.
- 13 Andersson, C. and Engardt, M.: European ozone in a future climate – the importance of
14 changes in dry deposition and isoprene emissions, *J. Geophys. Res.* 115,
15 doi:10.1029/2008JD011690, 2010.
- 16 Andersson, C., Bergström, R., Bennet, C., Robertson, L., Thomas, M., Korhonen, H.,
17 Lehtinen, K. E. J., and Kokkola, H.: MATCH-SALSA – Multi-scale Atmospheric Transport
18 and CHemistry model coupled to the SALSA aerosol microphysics model – Part 1: Model
19 description and evaluation, *Geosci. Model Dev.*, 8, 171-189, doi:10.5194/gmd-8-171-2015,
20 2015.
- 21 Carter, W. P.: Condensed atmospheric photooxidation mechanisms for isoprene, *Atmos.*
22 *Environ.* 30, 4275-4290, 1996.
- 23 Cooper, O. R., Parrish, D. D., Ziemke, J., Cupeiro, M., Galbally, I. E., Gilge, S., Horowitz, L.,
24 Jensen, N. R., Lamarque, J.-F., Naik, V., Oltmans, S. J., Schwab, J., Shindell, D. T.,
25 Thompson, A. M., Thouret, V., Wang, Y., and Zbinden, R.M.: Global distribution and trends
26 of tropospheric ozone: an observation-based review, *Elementa: science of the antropocene*, 2,
27 000029, 1-28, doi: 10.12952/journal.elementa.000029, 2014.
- 28 Courtier, P., Thépaut, J.-N. and Hollingsworth, A.: A strategy for operational implementation
29 of 4D-Var, using an incremental approach, *Q. J. Roy. Meteor. Soc.* 120, 1367-1388, 1994.



- 1 Dee, D. P., Uppala, S., Simmons, A., Berrisford, P., Poli, P., Kobayashi, S., Andrae, U.,
2 Balmaseda, A., Balsamo, G., Bauer, P., Bechtold, P., Beljaars, A. C. M., van de Berg, L.,
3 Bidlot, J.-R., Bormann, N., Delsol, C., Dragani, R., Fuentes, M., Geer, A., Haimberger, L.,
4 Healy, S., Hersbach, H., Hólm, E. V., Isaksen, L., Kållberg, P. W., Köhler, M., Matricardi,
5 M., McNally, A., Monge-Sanz, B. M., Morcrette, J.-J., Park, B.-K., Peubey, C., De Rosnay,
6 P., Tavolato, C., Thepaut, J.-J., and Vitart, F.: The ERA-Interim reanalysis: configuration and
7 performance of the data assimilation system, *Quart. J. Roy. Meteor. Soc.*, 137, 656, 553-597,
8 2011.
- 9 Denby, B. and Spangl, W.: The combined use of models and monitoring for applications
10 related to the European air quality directive: a working sub-group of FAIRMODE,
11 Proceedings of the HARMO13 conference, Paris, France, June 2010, H13-261, available at
12 internet URL:
13 [http://fairmode.jrc.ec.europa.eu/document/fairmode/event/presentation/20100601-h13-](http://fairmode.jrc.ec.europa.eu/document/fairmode/event/presentation/20100601-h13-261.pdf)
14 [261.pdf](http://fairmode.jrc.ec.europa.eu/document/fairmode/event/presentation/20100601-h13-261.pdf) (last access March, 2017), 2010.
- 15 Derwent R. G., Simmonds, P. G., Manning, A. J., and Spain, T.G.: Trends over a 20-year
16 period from 1987 to 2007 in surface ozone at the atmospheric research station, Mace Head,
17 Ireland, *Atmos. Environ.*, 41, 9091-9098, 2007.
- 18 Derwent, R. G., Manning, A. J., Simmonds, P. G., and Spain, T. G.: Analysis and
19 interpretation of 25 years of ozone observations at the Mace Head Atmospheric Research
20 Station on the Atlantic Ocean coast of Ireland from 1987 to 2012, *Atmos. Environ.*, 80, 361-
21 368, 2013.
- 22 Derwent, R. G., Utembe, S. R., Jenkin, M. E., and Shallcross, D.E.: Tropospheric ozone
23 production regions and the intercontinental origins of surface ozone over Europe, *Atmos.*
24 *Environ.*, 112, 216-224, 2015.
- 25 Engardt, M., Bergström, R., and Andersson, C.: Climate and emissions changes contributing
26 to changes in near-surface ozone in Europe over the coming decades – Results from model
27 studies, *Ambio*, 38, 452-458, 2009.
- 28 Engardt, M., Simpson, D., Schwikowski, M. and Granat, L.: Deposition of sulphur and
29 nitrogen in Europe 1900-2050. Model calculations and comparison to historical observations,
30 submitted to *Tellus*, 2017.



- 1 EU directive 2008/50/EC: directive 2008/50/EC of the European parliament and of the
2 council of 21 May 2008 on ambient air quality and cleaner air for Europe, Official Journal of
3 the European Union, 44pp, available at internet URL:
4 http://ec.europa.eu/environment/air/quality/legislation/existing_leg.htm (last access March,
5 2017), 11 June, 2008,
- 6 Finlayson-Pitts, B.J. and Pitts, J.N.: Chemistry of the upper and lower atmosphere. Theory,
7 experiments and applications, Academic press, California, USA, 969pp, ISBN: 0-12-257060,
8 2000.
- 9 Fusco, A. C. and Logan, J. A.: Analysis of 1970–1995 trends in tropospheric ozone at
10 Northern Hemisphere midlatitudes with the GEOS-CHEM model, *J Geophys. Res.*, 108, D15,
11 4449. doi: 10.1029/2002JD002742, 2003.
- 12 Gaudel, A., Ancellet, G., and Godin-Beekmann, S.: Analysis of 20 years of tropospheric
13 ozone vertical profiles by lidar and ECC at Observatoire de Haute Provence (OHP) at 44°N,
14 6.7°E, *Atmos. Environ.*, 113, 78-89, doi: 10.1016/j.atmosenv.2015.04.028, 2015.
- 15 Granier, C., Bessagnet, B., Bond, T., D’Angiola, A., Denier van der Gon, H., Frost, G. J.,
16 Heil, A., Kaiser, J. W., Kinne, S., Klimont, Z., Kloster, S., Lamarque, J.-F., Liousse, C.,
17 Masui, T., Meleux, F., Mieville, A., Ohara, T., Raut, J.-C., Riahi, K., Schultz, M. G., Smith,
18 S. J., Thompson, A., van Aardenne, J., van der Werf, G. R., and van Vuuren D. P.: Evolution
19 of anthropogenic and biomass burning emissions of air pollutants at global and regional scales
20 during the 1980–2010 period, *Climatic change* 109, 163-190, doi: 10.1007/s10584-011-0154-
21 1, 2011.
- 22 Hess, P. G. and Zbinden, R.: Stratospheric impact on tropospheric ozone variability and
23 trends: 1990-2009, *Atmos. Chem. Phys.*, 13, 649-674, doi:10.5194/acp-13-649-2013, 2013.
- 24 Inness, A., Baier, F., Benedetti, A., Bouarar, I., Chabrillat, S., Clark, H., Clerbaux, C.,
25 Coheur, P., Engelen, R. J., Errera, Q., Flemming, J., George, M., Granier, C., Hadji-Lazaro,
26 J., Huijnen, V., Hurtmans, D., Jones, L., Kaiser, J. W., Kapsomenakis, J., Lefever, K., Leitão,
27 J., Razinger, M., Richter, A., Schultz, M. G., Simmons, A. J., Suttie, M., Stein, O., Thépaut,
28 J.-N., Thouret, V., Vrekoussis, M., Zerefos, C., and the MACC team: The MACC reanalysis:
29 an 8 yr data set of atmospheric composition, *Atmos. Chem. Phys.*, 13, 4073-4109,
30 doi:10.5194/acp-13-4073-2013, 2013.



- 1 IPCC: Climate Change 2013. The physical Science Basis. IPCC Working group I contribution
2 to the AR5, Stocker, T.F., Qin, D., Plattner, G.K., Tignor, M.M.B., Allen, S.K., Boschung, J.,
3 Nauels, A., Xia, Y., Bex, V. and Midgley, P.M. (eds.), Cambridge University Press,
4 Cambridge, United Kingdom and New York, NY, USA, 1535pp, available at internet URL:
5 http://www.climatechange2013.org/images/report/WGIAR5_ALL_FINAL.pdf (last access
6 March, 2017), 2013.
- 7 Jacob, D. J., Logan, J. A., Yevich, R. M., Gardner, G. M., Spivakovsky, C. M., Wofsy, S. C.,
8 Munger, J. W., Sillman, S., Prather, M. J., Rodgers, M. O., Westberg, H., and Zimmerman, P.
9 R.: Simulation of summertime ozone over North-America. *J. Geophys. Res.* 98, D8, 14797-
10 14816, doi: 10.1029/93JD01223, 1993.
- 11 Jonson, J. E., Simpson, D., Fagerli, H., and Solberg, S.: Can we explain the trends in
12 European ozone levels?, *Atmos. Chem. Phys.*, 6, 51-66, doi:10.5194/acp-6-51-2006, 2006.
- 13 Kalnay, E.: Atmospheric modeling, data assimilation and predictability. Cambridge
14 University Press, Cambridge and New York, USA, ISBN 0-521-79629-6, 2003.
- 15 Karlsson, P. E., Klingberg, J., Engardt, M., Andersson, C., Langner, J., Pihl Karlsson, G., and
16 Pleijel, H.: Past, present and future concentrations of ground-level ozone and potential
17 impacts on ecosystems and human health in northern Europe, *Sci. Tot. Environ.*, 576, 22-35,
18 doi: 10.1016/j.scitotenv.2016.10.061, 2017.
- 19 Katragkou, E., Zanis, P., Tsikerdekis, A., Kapsomenakis, J., Melas, D., Eskes, H., Flemming,
20 J., Huijnen, V., Inness, A., Schultz, M. G., Stein, O., and Zerefos, C. S.: Evaluation of near-
21 surface ozone over Europe from the MACC reanalysis, *Geosci. Model Dev.*, 8, 2299-2314,
22 doi:10.5194/gmd-8-2299-2015, 2015.
- 23 Klingberg, J., Björkman, M. P., Pihl Karlsson, G., and Pleijel, H.: Observations of Ground-
24 level Ozone and NO₂ in Northernmost Sweden, Including the Scandian Mountain Range,
25 *Ambio*, 38, 448-541, 2009.
- 26 Klingberg J., Karlsson P. E., Pihl Karlsson G., Hu Y., Chen D., and Pleijel H.: Variation in
27 ozone exposure in the landscape of southern Sweden with consideration of topography and
28 coastal climate, *Atmos. Environ.*, 47, 252-260, 2012.
- 29 Kumar, A., Wu, S., Weise, M. F., Honrath, R., Owen, R. C., Helmig, D., Kramer, L., Val
30 Martin, M., and Li, Q.: Free-troposphere ozone and carbon monoxide over the North Atlantic



- 1 for 2001–2011, Atmos. Chem. Phys., 13, 12537-12547, doi:10.5194/acp-13-12537-2013,
2 2013.
- 3 Lacressoniere, G., Foret, G., Beekman, M., Siour, G., Engardt, M., Gauss, M., Watson, L.,
4 Andersson, C., Colette, A., Josse, B., Macreca, V., Nyirui, A., and Vautard, R.: Impacts of
5 regional climate change on air quality projections and associated uncertainties, Climatic
6 change, 136, 309-324, doi: 10.1007/s10584-016-1619-z, 2016.
- 7 Lamarque, J.-F., Bond, T. C., Eyring, V., Granier, C., Heil, A., Klimont, Z., Lee, D., Liousse,
8 C., Mieville, A., Owen, B., Schultz, M. G., Shindell, D., Smith, S. J., Stehfest, E., Van
9 Aardenne, J., Cooper, O. R., Kainuma, M., Mahowald, N., McConnell, J. R., Naik, V., Riahi,
10 K., and van Vuuren, D. P.: Historical (1850–2000) gridded anthropogenic and biomass
11 burning emissions of reactive gases and aerosols: methodology and application, Atmos.
12 Chem. Phys., 10, 7017-7039, doi:10.5194/acp-10-7017-2010, 2010.
- 13 Langner, J., Bergström, R., and Pleijel, K.: European scale modeling of sulfur, oxidised
14 nitrogen and photochemical oxidants. Model development and evaluation for the 1994
15 growing season, Swedish Meteorological and Hydrological Institute, Norrköping, Sweden,
16 SMHI RMK No. 82, 71 pp. (with errata), available at internet URL:
17 http://www.smhi.se/polopoly_fs/1.35257!/RMK82.pdf (last access March, 2017), 1998.
- 18 Langner, J., Engardt, M., and Andersson, C.: European summer surface ozone 1990–2100,
19 Atmos. Chem. Phys., 12, 10097-10105, doi:10.5194/acp-12-10097-2012, 2012.
- 20 Lefohn, A. S., Malley, C. S., Simon, H., Wells, B., Xu, X., Zhang, L., and Wang, T.:
21 Responses of human health and vegetation exposure metrics to changes in ozone
22 concentration distributions in the European Union, United States and China, Atmos. Environ.
23 152, 123-145, doi: 10.1016/j.atmosenv.2016.12.025, 2017.
- 24 Lelieveld, J. and Dentener, F. J.: What controls tropospheric ozone? J. Geophys. Res., 105,
25 3531-3551, doi: 10.1029/1999JD901011, 2000.
- 26 Logan, J. A., Staehelin, J., Megretskaia, I. A., Cammas, J. P., Thouret, V., Claude, H., de
27 Backer, H., Steinbacher, M., Scheel, H. E., Stübi, R., Fröhlich, M., and Derwent, R.: Changes
28 in ozone over Europe: Analysis of ozone measurements from sondes, regular aircraft
29 (MOZAIC) and alpine surface sites, J. Geophys. Res. 117, D09301,
30 doi:10.1029/2011JD016952, 2012.



- 1 Markakis, K., Valari, M., Engardt, M., Lacressonniere, G., Vautard, R., and Andersson, C.:
2 Mid-21st century air quality at the urban scale under the influence of changed climate and
3 emissions – case studies for Paris and Stockholm, Atmos. Chem. Phys., 16, 1877-1894,
4 doi:10.5194/acp-16-1877-2016, 2016.
- 5 Miyazaki, K., Eskes, H. J., and Sudo, K.: A tropospheric chemistry reanalysis for the years
6 2005–2012 based on an assimilation of OMI, MLS, TES, and MOPITT satellite data, Atmos.
7 Chem. Phys., 15, 8315-8348, doi:10.5194/acp-15-8315-2015, 2015.
- 8 Monks, P.S., Archibald, A.T., Colette, A., Cooper, O., Coyle, M., Derwent, R., Fowler, D.,
9 Granier, C., Law, K.S., Mills, G.E., Stevenson, D.S., Tarasova, O., Thouret, V., von
10 Schneidenmesser, E., Sommariva, R., Wild, O., and Williams, M.L.: Tropospheric ozone and
11 its precursors from the urban to the global scale from air quality to short-lived climate forcer,
12 Atmos. Chem. Phys. 15, 8889-8973, doi:10.5194/acp-15-8889-2015, 2015.
- 13 NV: Internet URL: [http://www.naturvardsverket.se/en/Environmental-objectives-and-](http://www.naturvardsverket.se/en/Environmental-objectives-and-cooperation/Swedens-environmental-objectives/The-national-environmental-objectives/Clean-Air/Specifications-for-Clean-Air/)
14 [cooperation/Swedens-environmental-objectives/The-national-environmental-](http://www.naturvardsverket.se/en/Environmental-objectives-and-cooperation/Swedens-environmental-objectives/The-national-environmental-objectives/Clean-Air/Specifications-for-Clean-Air/)
15 [objectives/Clean-Air/Specifications-for-Clean-Air/](http://www.naturvardsverket.se/en/Environmental-objectives-and-cooperation/Swedens-environmental-objectives/The-national-environmental-objectives/Clean-Air/Specifications-for-Clean-Air/) Last accessed 21 March, 2017.
- 16 Ohara, T., Akimoto, H., Kurokawa, J., Horii, N., Yamaji, K., Yan, X., and Hayasaka, T.: An
17 Asian emission inventory of anthropogenic emission sources for the period 1980–2020,
18 Atmos. Chem. Phys., 7, 4419-4444, doi:10.5194/acp-7-4419-2007, 2007.
- 19 Oltmans, S.J., Lefohn, A.S., Harris, J.M., Galbally, I., Scheel, H.E., Bodeker, G., Brunke, E.,
20 Claude, H., Tarasick, D., Johnson, B.J., Simmonds, P., Shadwick, D., Anlauf, K., Hayden, K.,
21 Schmidlin, F., Fujimoto, T., Akagi, K., Meyer, C., Nichol, S., Davies, J., Redondas, A. and
22 Cuevaso, E.: Long-term changes in tropospheric ozone, Atmos. Environ., 40, 3156-3173,
23 2006.
- 24 Parrish, D. D., Law, K. S., Staehelin, J., Derwent, R., Cooper, O. R., Tanimoto, H., Volz-
25 Thomas, A., Gilge, S., Scheel, H.-E., Steinbacher, M., and Chan, E.: Long-term changes in
26 lower tropospheric baseline ozone concentrations at northern mid-latitudes, Atmos. Chem.
27 Phys., 12, 11485-11504, doi:10.5194/acp-12-11485-2012, 2012.
- 28 Parrish, D.D., Law, K.S., Staehelin, J., Derwent, R., Cooper, O.R., Tanimoto, H., Volz-
29 Thomas, A., Gilge, S., Scheel, H.-E., Steinbacher, M. and Chan, E.: Lower tropospheric
30 ozone at northern midlatitudes: changing seasonal cycle, Geophys. Res. Lett., 40, 1631-1636,
31 doi: 10.1002/grl.50303, 2013.



- 1 Parrish, D. D., Lamarque, J.-F., Naik, V., Horowitz, L., Shindell, D. T., Staehelin, J.,
2 Derwent, R., Cooper, O. R., Tanimoto, H., Volz-Thomas, A., Gilge, S., Scheel, H.-E.,
3 Steinbacher, M. and Fröhlich, M.: Long-term changes in lower tropospheric baseline ozone
4 concentrations: Comparing chemistry-climate models and observations at northern
5 midlatitudes, *J Geophys. Res. Atmos.*, 119, 5719–5736, doi:10.1002/2013JD021435, 2014.
- 6 Pozzoli, L., Janssen-Maenhout, G., Diehl, T., Bey, I. Schultz, M. G., Feichter, J., Vignati, E.
7 and Dentener F.: Re-analysis of tropospheric sulfate aerosol and ozone for the period 1980–
8 2005 using the aerosol-chemistry-climate model ECHAM5-HAMMOZ, *Atmos. Chem. Phys.*,
9 11, 9563-9594, doi: 10.5194/acp-11-9563-2011, 2011.
- 10 Robertson, L., Langner, J. and Engardt, M.: An Eulerian limited-area atmospheric transport
11 model, *J. Appl. Meteor.*, 38, 190-210, 1999.
- 12 Robertson, L. and Kahnert, M.: 2D variational data assimilation of near surface chemical
13 species, Borrego, C. and Renner, E. (eds), *Air pollution modelling and its application XVIII*,
14 Elsevier, Amsterdam, 2007.
- 15 Robichaud, A. and Ménard, R.: Multi-year objective analyses of warm season ground-level
16 ozone. *Atmos. Chem. Phys.*, 14, 1769-1800, 2014.
- 17 Royal Society: Ground level ozone in the 21st century: future trends, impacts and policy
18 implications, Science Policy report 15/08, the royal society, London, UK, available online at
19 internet URL:
20 https://royalsociety.org/~media/Royal_Society_Content/policy/publications/2008/7925.pdf
21 (last access March, 2017), 2008.
- 22 Schultz, M.G., Backman, L., Balkanski, Y., Bjoerndalsaeter, S., Brand, R., Burrows, J.P.,
23 Dalsoeren, S., de Vasconcelos, M., Grodtmann, B., Hauglustaine, D.A., Heil, A.,
24 Hoelzemann, J.J., Isaksen, I.S.A., Kaurola, J., Knorr, W., Ladstaetter-Weissenmayer, A.,
25 Mota, B., Oom, D., Pacyna, J., Panasiuk, D., Pereira, J.M.C., Pulles, T., Pyle, J., Rast, S.,
26 Richter, A., Savage, N., Schnadt, C., Schulz, M., Spessa, A., Staehelin, J., Sundet, J.K.,
27 Szopa, S., Thonicke, K., van het Bolscher, M., van Noije, T., van Velthoven, P., Vik, A.F. and
28 Wittrock, F.: Reanalysis of the Tropospheric chemical composition over the past 40 years
29 (RETRO) – a long-term global modeling study of tropospheric chemistry, Final report,
30 Schultz, M.G. (ed.), Reports on Earth System Science, 48/2007, Max Planck Institute for
31 Meteorology, Hamburg, Germany, available at internet URL:



- 1 https://www.mpimet.mpg.de/fileadmin/publikationen/Reports/WEB_BzE_48.pdf (last access:
2 March 2017), 2007.
- 3 Simmonds, P.G., Derwent, R.G., Manning, A.L. and Spain, G.: Significant growth in surface
4 ozone at Mace Head, Ireland, 1987-2003, *Atmos. Environ.*, 38, 4769-4778, 2004.
- 5 Simon, H., Reff, A., Wells, B., Xing, J. and Frank, N.: Ozone trends across the United States
6 over a period of decreasing NO_x and VOC emissions, *Environ. Sci. Technol.*, 49, 186-195.
7 doi: 10.1021/es504514z, 2015..
- 8 Simpson, D., Guenther, A., Hewitt, C.N. and Steinbrecher, R.: Biogenic emissions in Europe:
9 1. Estimates and uncertainties, *J. Geophys. Res. Atmos.*, 100, D11, 22875-22890, 1995.
- 10 Simpson, D., Benedictow, A., Berge, H., Bergström, R., Emberson, L. D., Fagerli, H.,
11 Flechard, C. R., Hayman, G. D., Gauss, M., Jonson, J. E., Jenkin, M. E., Nyíri, A., Richter,
12 C., Semeena, V. S., Tsyro, S., Tuovinen, J.-P., Valdebenito, Á., and Wind, P.: The EMEP
13 MSC-W chemical transport model – technical description, *Atmos. Chem. Phys.*, 12, 7825-
14 7865, doi:10.5194/acp-12-7825-2012, 2012.
- 15 Simpson, D., Arneth, A., Mills, G., Solberg, S. and Uddling, J.: Ozone – the persistent
16 menace: interactions with the N cycle and climate change, *Current opinion in Environ.*
17 *Sustainability*, 9, 9-19, 2014.
- 18 Verstraeten, W.W., Neu, J.L., Williams, J.E., Bowman, K.W., Worden, J.R. and Folkert
19 Boersma, K.: Rapid increases in tropospheric ozone production and export from China.
20 *Nature geoscience* 8, 690-697, 2015.
- 21 Watson, L., Lacrosoniere, G., Gauss, M., Engardt, M., Andersson, C., Josse, B., Marecal, V.,
22 Nyiri, A., Sobolowski, S., Siour, G. and Vautard, R.: The impact of meteorological forcings
23 on gas phase air pollutants over Europe. *Atmos. Environ.* 119, 240-257, 2015.
- 24 Watson, L., Lacrosonnire, G., Gauss, M., Engardt, M., Andersson, C., Josse, B., Marcal, V.,
25 Nyiri, A., Sobolowski, S., Szopa, S., Siour, G. and Vautard, R.: Impact of emissions and +2°C
26 climate change upon future ozone and nitrogen dioxide over Europe, *Atmos. Environ.*, 142,
27 271-285, doi:10.1016/j.atmosenc.2016.07.051, 2016.
- 28 WHO: WHO Air quality guidelines for particulate matter, ozone, nitrogen dioxide and sulfur
29 dioxide. Global update 2005. Summary of risk assessment, WHO press, World Health
30 Organization, Geneva, Switzerland, available online at internet URL



- 1 http://www.who.int/phe/health_topics/outdoorair/outdoorair_aqg/en/ (last access March,
- 2 2017), 2006.
- 3 Xing, J., Mathur, R., Pleim, J., Hogrefe, C., Gan, C.-M., Wong, D.C., Wei, C., Gilliam, R.
- 4 and Pouliot, G.: Observations and modeling of air quality trends over 1990-2010 across the
- 5 northern hemisphere: China, the United States and Europe., Atmos. Chem. Phys., 15, 2723-
- 6 2747, doi:10.5194/acp-15-2723-2015, 2015.
- 7 Zanis, P., Hadjinicolaou, P., Pozzer, A., Tyrllis, E., Dafka, S., Mihalopoulos, N. and Lelieveld,
- 8 J.: Summertime free-tropospheric ozone pool over the eastern Mediterranean/Middle East,
- 9 Atmos. Chem. Phys., 14, 115-132. doi: 10.5194/acp-14-115-2014, 2014..
- 10 Zhang, Y. Bocquet, M., Mallet, V., Seigneur, C. and Baklanov, A.: Real-time air quality
- 11 forecasting, part II: State of the science, current research needs, and future prospects, Atmos.
- 12 Environ., 60, 656-676, doi: 10.1016/j.atmosenv.2012.02.041, 2012.
- 13
- 14



1 **Figure and table legends**

2 **Figure legends**

3 Figure 1. A flow-chart of the relevant part of the MATCH Sweden system for this reanalysis
4 study.

5 Figure 2. (a) Secular trend of factors used for scaling boundary concentration of relevant
6 species. Note that the hemispheric background ozone concentrations are assumed constant
7 from 2000 onwards. CO and NMVOC boundaries are held constant throughout the
8 simulation. (b) Temporal trend of total domain (solid lines; left vertical scale) and Swedish
9 (dashed lines; right vertical scale) annual O₃ precursor emissions utilized by MATCH from
10 1990 to 2013. Emissions of nitrogen oxides (NO_x), non-methane volatile organic compounds
11 (NMVOC), carbon monoxide (CO) and biogenic isoprene (C₅H₈) are indicated by different
12 colors (cf. legend); emissions of sulfur oxides (SO_x) and ammonia (NH₃) are excluded from
13 the panel.

14 Figure 3. Instrumentation sites for hourly near-surface ozone concentration observations in
15 Sweden and Norway, which are used in the variational analysis. Red circles: sites with full
16 data coverage. Blue circles: sites with restricted data coverage. The subdivision of Sweden
17 into three regions (North, Central and South) follows county borders, as indicated by the fat
18 black lines.

19 Figure 4. Data availability at instrumentation sites for hourly near-surface ozone
20 concentration observations in Sweden and Norway. Red squares: years with at least 80 %
21 annual data for sites with full data coverage (see also Fig. 3). Light red: sites with <80 %
22 annual data (data capture indicated in square) for sites with full coverage. Blue and light blue
23 squares: as for the red squares, but for sites with restricted data coverage.

24 Figure 5. Trends in near-surface ozone percentile levels averaged for the three regions North
25 (blue), Central (green) and South (magenta) for the sum of the contributions to the trend
26 (SUM) vs the MATCH model simulation MFG (a) and the MATCH model simulation MFG
27 vs the reanalysis LONGTERM (b). Filled circles indicate significant trends ($p \leq 0.05$) in the
28 MFG simulation, whereas non-significant MFG trends ($p > 0.5$) are indicated by an empty
29 circle. 1:1 line in black, factor 2 lines in dark grey and equal sign quadrants are separated by
30 light grey lines.



1 Figure 6. Seasonal cycle of monthly mean (a) and monthly maximum of 1h mean (b) near-
2 surface ozone concentrations averaged over the period 1990-2013 (solid lines; left vertical
3 scale) and the linear trend over the same period of the respective monthly values (dashed
4 lines; right vertical scale) in the three regions North, Central and South Sweden (cf. Fig. 3).
5 The corresponding regions are referred to by different colors, see legend. Results from the
6 LONGTERM reanalysis.

7 Figure 7. Statistical properties of the annual mean (top row; (a)-(e)) and annual maximum 1h
8 mean (bottom row; ((f)-(j)) near-surface ozone concentration. In the columns from left to
9 right: 1990-2013 mean ((a),(f)), 1990-2013 maximum ((b),(g)), 1990-2013 standard deviation
10 ((c),(h)), linear trend over the period 1990-2013 ((d),(i)) and significance in the linear trend
11 over the period ((e),(j)). Results from the LONGTERM reanalysis.

12 Figure 8. Temporal variation of annual percentiles of near-surface ozone concentrations
13 averaged over the three regions North (a), Central (b) and South (c) of Sweden (cf. Fig. 3).
14 The line marked 0 is the zero-percentiles (lowest hourly mean near-surface ozone
15 concentration of the year), 100 is 100-percentile (highest hourly mean near-surface ozone
16 concentration of the year), 50 is the 50-percentile (i.e. annual median of the hourly mean near-
17 surface ozone concentration). The sign of the corresponding linear trend (cf. Supplements
18 Table S3, including a statistical analysis of the trend) of each percentile is indicated by colour:
19 a negative linear trend over 1990-2013 is indicated by grey symbols; a positive trend by
20 orange symbols. Statistically significant trends ($p \leq 0.05$) are indicated by thick lines. Results
21 from the LONGTERM reanalysis.

22 Figure 9. Linear trend over 1990-2013 in monthly mean ((a),(c)) and monthly maximum 1
23 hour mean ((b),(d)) near-surface ozone concentration for the North ((a),(b)) and the South
24 ((c),(d)) Swedish regions (cf. Fig. 3). Reanalyzed (white diamond; LONGTERM reanalysis)
25 and modelled “first guess” (MFG) near-surface ozone trend (green diamond), and modelled
26 contributions to the near-surface ozone trend due to change in emissions: anthropogenic
27 Swedish (dark blue, Se emis) and full domain, non-Swedish (fair blue, Eur emis), emissions,
28 trend in top and lateral boundaries of relevant species (yellow, bound) and variation in
29 meteorology (brown, meteo). The sum of the modelled contributions is indicated by the
30 dashed green line.

31 Figure 10. Linear trends over 1990-2013 in annual percentiles of hourly mean near-surface
32 ozone concentrations for the North (a) and the South (b) Sweden regions. Reanalyzed (white



1 diamond; LONGTERM reanalysis) and modelled MFG near-surface ozone trend (green
2 diamond), and modelled contributions to the near-surface ozone concentration trend due to
3 change in emissions: anthropogenic Swedish (dark blue, Se emis) and full domain, non-
4 Swedish (fair blue, Eur emis), emissions, trend in top and lateral boundaries of relevant
5 species (yellow, bound) and variation in meteorology (brown, meteo). The sum of the
6 modelled contributions is indicated by the dashed green line.

7

8



1 **Table legends**

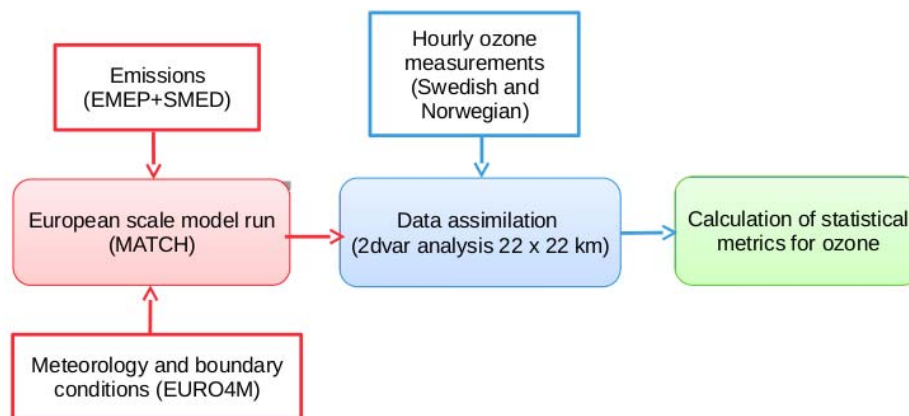
2 Table 1a. Model calculations and scenarios, all covering the years 1990-2013, including the
3 “first guess” to the data assimilation and base case to the sensitivity simulations (MFG), two
4 reanalysis data sets (LONGTERM and ALL), sensitivity scenarios (MEUR, MSE, MBC and
5 MMET).

6 Table 1b. Formation of contributions to the linear trend over the period 1990-2013 from the
7 sensitivity simulations (Se emis, Eur emis, Bound and Meteo, see Table 1a).

8 Table 2. Evaluation of modelled hourly near-surface ozone concentrations in 2013 at Swedish
9 observation sites. Mean value (mean), standard deviation (σ), model mean bias normalized by
10 the observed mean (%bias), Pearson correlation coefficients (r) for data including at least 10
11 pairs, the root mean square error (RMSE) and number of observed hours at the sites. The
12 evaluation includes the reanalyzed data sets ALL and LONGTERM, where ALL is evaluated
13 at the 12 Swedish sites included in that simulation, and LONGTERM is evaluated at the 6
14 Swedish sites included in that simulation (cf. Fig. 4). For each of these data set evaluations we
15 include the observation *dependent* reanalysis (2dvar), the observation *independent* cross
16 validation of the reanalysis (cross) and the MATCH base case simulation (MFG). The top half
17 of the table shows the temporal performance (spatial mean of statistics, see Supplement Sect.
18 S1). The bottom half of the table shows spatial performance (spatial statistics of annual
19 means, see Supplement Sect. S1).

20 Table 3. Linear trend during 1990-2013 of policy related metrics in the 3 Swedish regions
21 North, Central and South (cf. Fig. 3). Stars (*, **, and ***) indicate that the trend is
22 significant ($p \leq 0.05$, $p \leq 0.01$, $p \leq 0.001$, respectively).

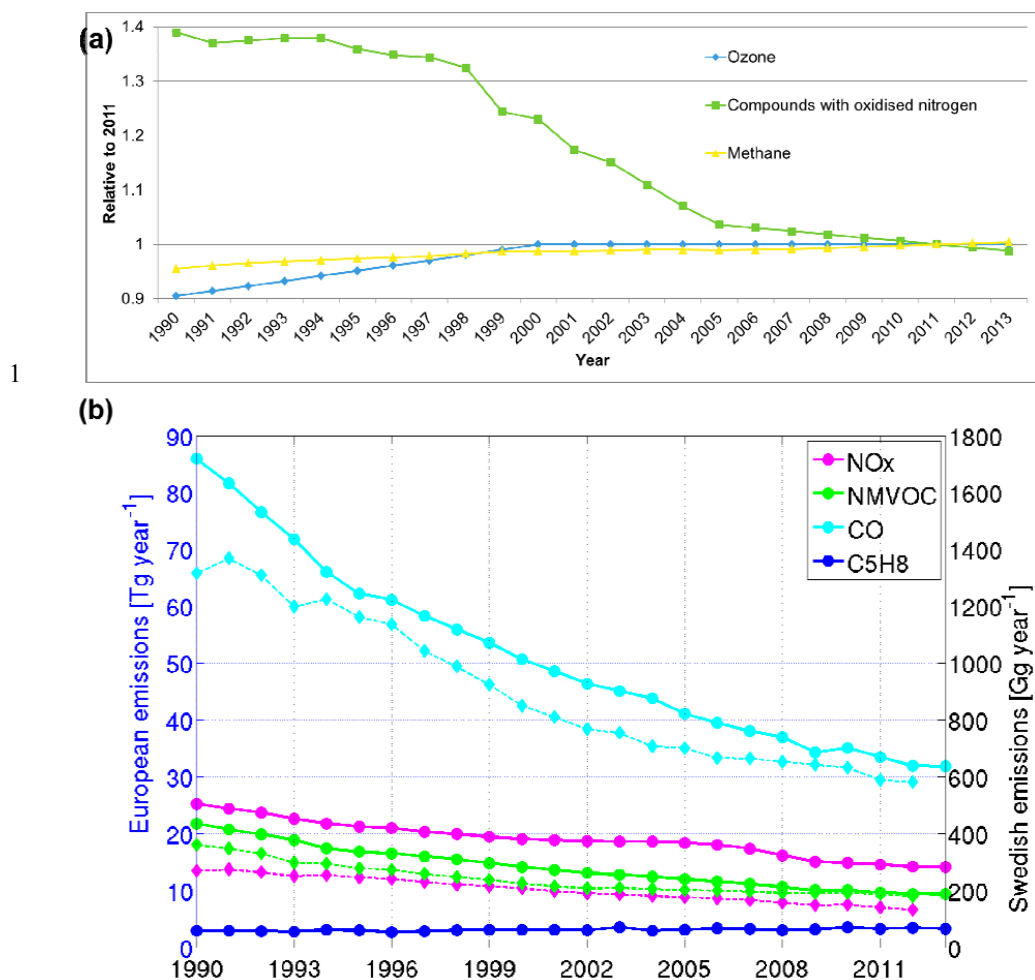
23



1

2 Figure 1. A flow-chart of the relevant part of the MATCH Sweden system for this reanalysis

3 study.



2

3 Figure 2. (a) Secular trend of factors used for scaling boundary concentration of relevant
4 species. Note that the hemispheric background ozone concentrations are assumed constant
5 from 2000 onwards. CO and NMVOC boundaries are held constant throughout the
6 simulation. (b) Temporal trend of total domain (solid lines; left vertical scale) and Swedish
7 (dashed lines; right vertical scale) annual O₃ precursor emissions utilized by MATCH from
8 1990 to 2013. Emissions of nitrogen oxides (NO_x), non-methane volatile organic compounds
9 (NMVOC), carbon monoxide (CO) and biogenic isoprene (C₅H₈) are indicated by different
10 colors (cf. legend); emissions of sulfur oxides (SO_x) and ammonia (NH₃) are excluded from
11 the panel.



1

2 Figure 3. Instrumentation sites for hourly near-surface ozone concentration observations in
3 Sweden and Norway, which are used in the variational analysis. Red circles: sites with full
4 data coverage. Blue circles: sites with restricted data coverage. The subdivision of Sweden
5 into three regions (North, Central and South) follows county borders, as indicated by the fat
6 black lines.

7



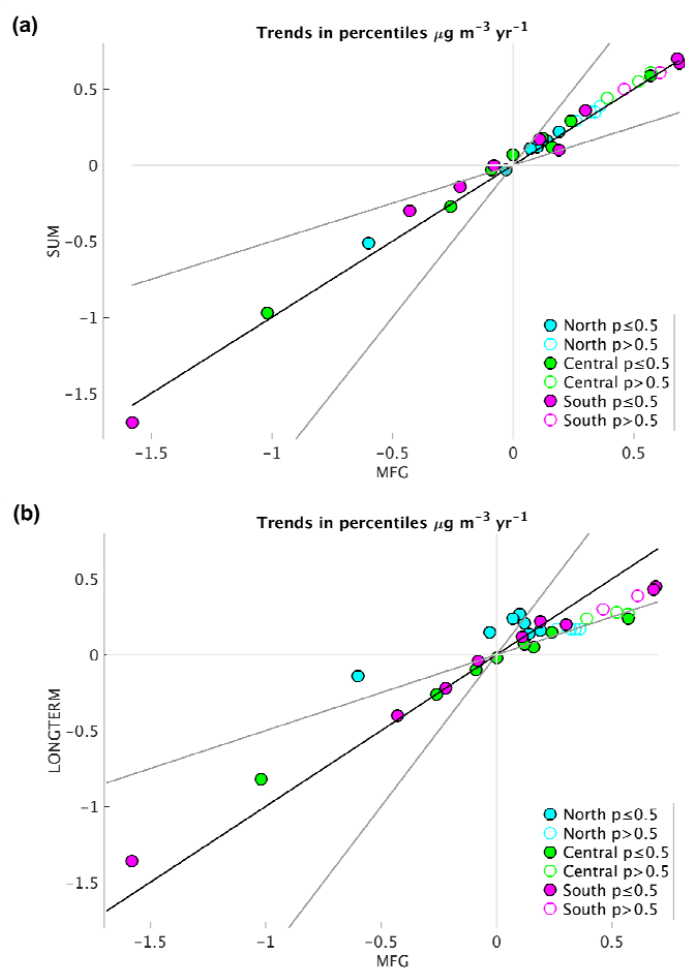
		1990	1991	1992	1993	1994	1995	1996	1997	1998	1999	2000	2001	2002	2003	2004	2005	2006	2007	2008	2009	2010	2011	2012	2013
SE13	Esränge	30																							
SE35	Vindeln																								
SE05	Bredkälen															58									
SE89	Grimsö											42													
NM	Norr Malma																0.01								
SE12	Aspvreten																								
SE32	Norra Kvill																								
SE88	Asa försökspark						50				75					45								58	
SE87	Östad												47	34	20	45	49	50	50	50	50	50	49	50	
SE02	Rörvik																								
SE14	Råö																								
RDB	Rödeby																								56
SE11	Vavihill																								
NO15	Tustervatn					73																			
NO39	Kårvatn																								
NO489	Haukenes		47	22	42	51	51	53	55	49	49	51	39	53	53		40		67				72		
NO43	Prestebakke				65																				
NO01	Birkenes I																								
NO02	Birkenes II																								79

1

2 Figure 4. Data availability at instrumentation sites for hourly near-surface ozone
 3 concentration observations in Sweden and Norway. Red squares: years with at least 80 %
 4 annual data for sites with full data coverage (see also Fig. 3). Light red: sites with <80 %
 5 annual data (data capture indicated in square) for sites with full coverage. Blue and light blue
 6 squares: as for the red squares, but for sites with restricted data coverage. White squares: no
 7 observations are available for that year and site. The LONGTERM reanalysis includes the red
 8 measurement sites, the ALL reanalysis includes both red and blue.

9

10



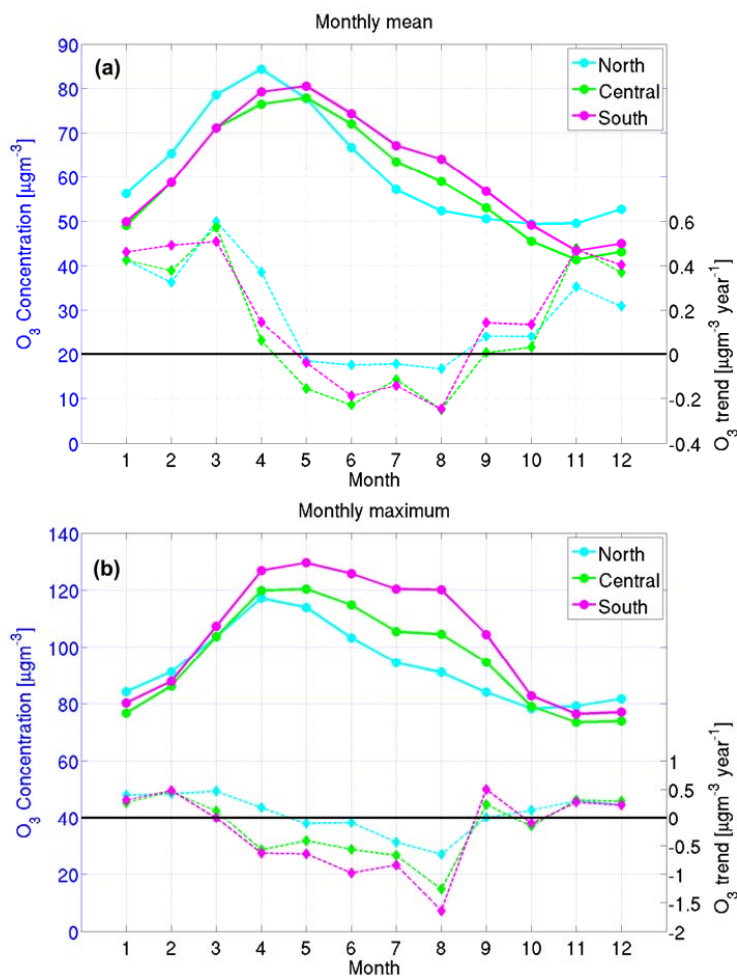
1

2

3 Figure 5. Trends in near-surface ozone percentile levels averaged for the three regions North
4 (blue), Central (green) and South (magenta) for the sum of the contributions to the trend
5 (SUM) vs the MATCH model simulation MFG (a) and the MATCH model simulation MFG
6 vs the reanalysis LONGTERM (b). Filled circles indicate significant trends ($p \leq 0.05$) in the
7 MFG simulation, whereas non-significant MFG trends ($p > 0.5$) are indicated by an empty
8 circle. 1:1 line in black, factor 2 lines in dark grey and equal sign quadrants are separated by
9 light grey lines.

10

11



1

2

3 Figure 6. Seasonal cycle of monthly mean (a) and monthly maximum of 1h mean (b) near-
4 surface ozone concentrations averaged over the period 1990-2013 (solid lines; left vertical
5 scale) and the linear trend over the same period of the respective monthly values (dashed
6 lines; right vertical scale) in the three regions North, Central and South Sweden (cf. Fig. 3).
7 The corresponding regions are referred to by different colors, see legend. Results from the
8 LONGTERM reanalysis.

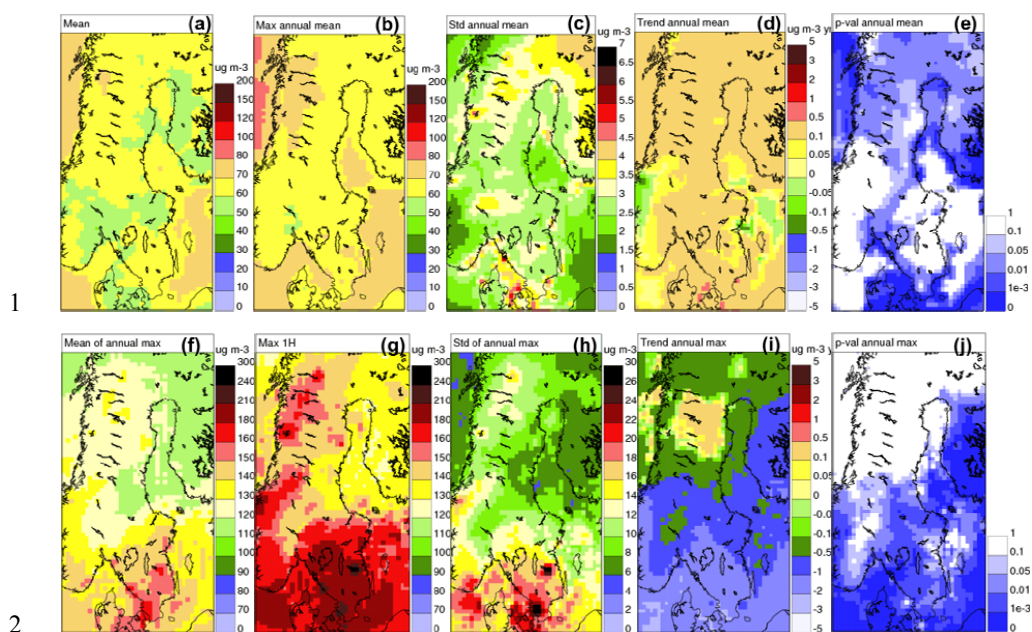
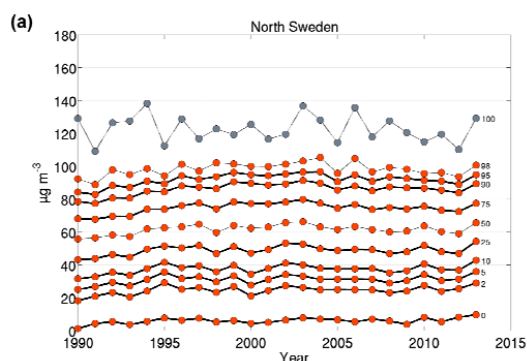


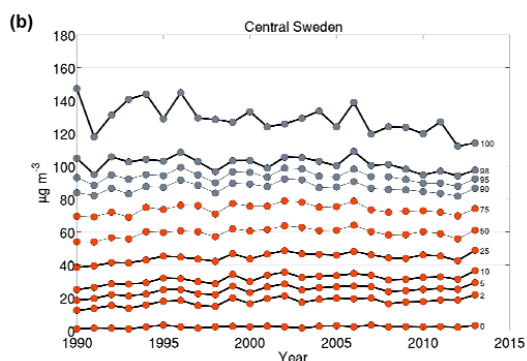
Figure 7. Statistical properties of the annual mean (top row; (a)-(e)) and annual maximum 1h mean (bottom row; ((f)-(j)) near-surface ozone concentration. In the columns from left to right: 1990-2013 mean ((a),(f)), 1990-2013 maximum ((b),(g)), 1990-2013 standard deviation ((c),(h)), linear trend over the period 1990-2013 ((d),(i)) and significance in the linear trend over the period ((e),(j)). Results from the LONGTERM reanalysis.



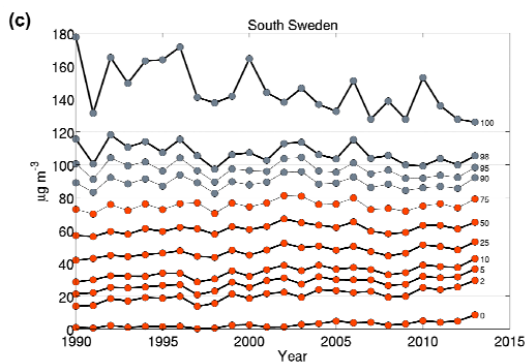
1



2



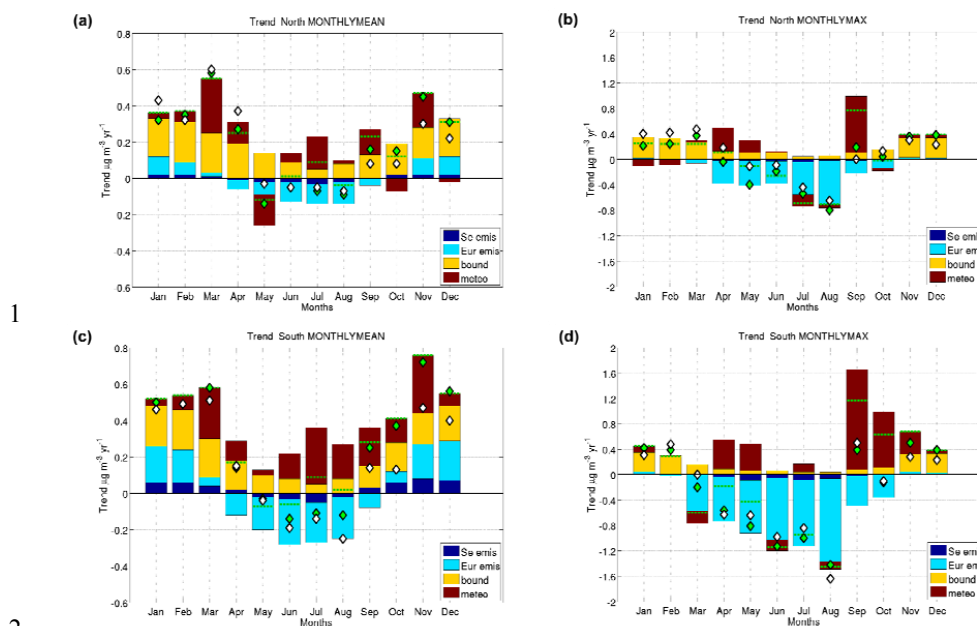
3



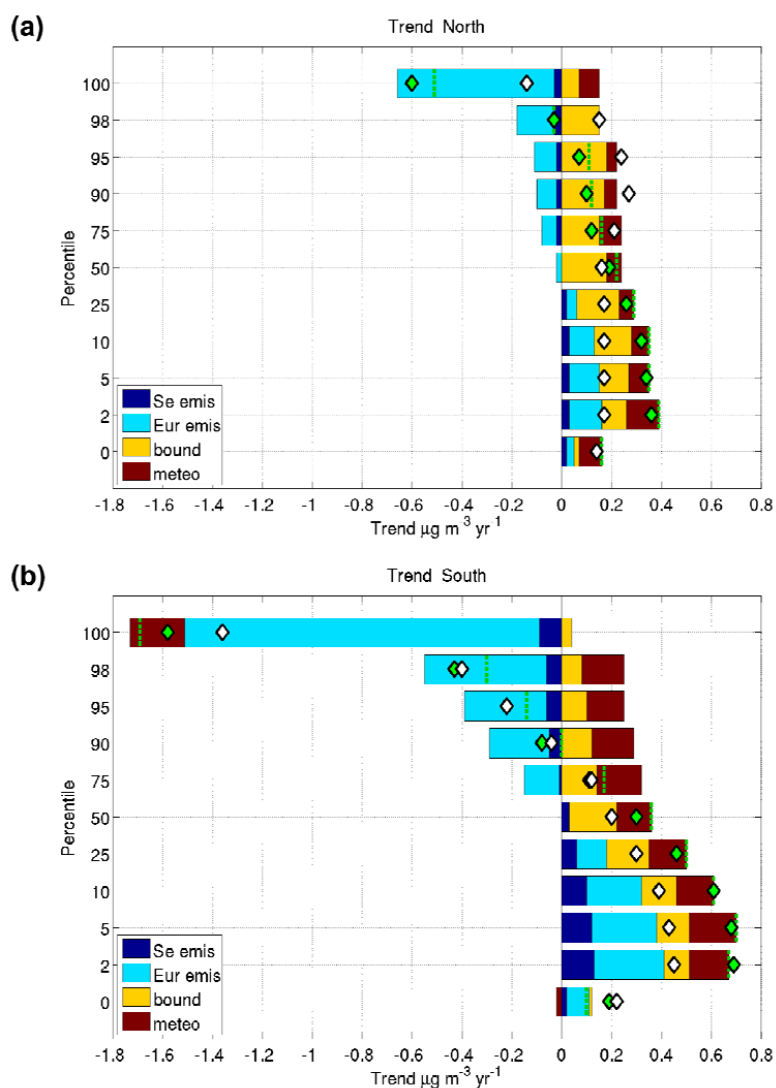
4 Figure 8. Temporal variation of annual percentiles of near-surface ozone concentrations
5 averaged over the three regions North (a), Central (b) and South (c) of Sweden (cf. Fig. 3).
6 The line marked 0 is the zero-percentiles (lowest hourly mean near-surface ozone
7 concentration of the year), 100 is 100-percentile (highest hourly mean near-surface ozone
8 concentration of the year), 50 is the 50-percentile (i.e. annual median of the hourly mean near-
9 surface ozone concentration). The sign of the corresponding linear trend (cf. Supplements
10 Table S3, including a statistical analysis of the trend) of each percentile is indicated by colour:



- 1 a negative linear trend over 1990-2013 is indicated by grey symbols; a positive trend by
- 2 orange symbols. Statistically significant trends ($p \leq 0.05$) are indicated by thick lines. Results
- 3 from the LONGTERM reanalysis.



1
 2
 3 Figure 9. Linear trend over 1990-2013 in monthly mean ((a),(c)) and monthly maximum
 4 hour mean ((b),(d)) near-surface ozone concentration for the North ((a),(b)) and the South
 5 ((c),(d)) Swedish regions (cf. Fig. 3). Reanalyzed (white diamond; LONGTERM reanalysis)
 6 and modelled “first guess” (MFG) near-surface ozone trend (green diamond), and modelled
 7 contributions to the near-surface ozone trend due to change in emissions: anthropogenic
 8 Swedish (dark blue, Se emis) and full domain, non-Swedish (fair blue, Eur emis), emissions,
 9 trend in top and lateral boundaries of relevant species (yellow, bound) and variation in
 10 meteorology (brown, meteo). The sum of the modelled contributions is indicated by the
 11 dashed green line.



1

2

3 Figure 10. Linear trends over 1990-2013 in annual percentiles of hourly mean near-surface
 4 ozone concentrations for the North (a) and the South (b) Sweden regions. Reanalyzed (white
 5 diamond; LONGTERM reanalysis) and modelled MFG near-surface ozone trend (green
 6 diamond), and modelled contributions to the near-surface ozone concentration trend due to
 7 change in emissions: anthropogenic Swedish (dark blue, Se emis) and full domain, non-
 8 Swedish (fair blue, Eur emis), emissions, trend in top and lateral boundaries of relevant



- 1 species (yellow, bound) and variation in meteorology (brown, meteo). The sum of the
- 2 modelled contributions is indicated by the dashed green line.
- 3



- 1 Table 1a. Model calculations and scenarios, all covering the years 1990-2013, including the
- 2 “first guess” to the data assimilation and base case to the sensitivity simulations (MFG), two
- 3 reanalysis data sets (LONGTERM and ALL), sensitivity scenarios (MEUR, MSE, MBC and
- 4 MMET).

Scenario/data set	Description
MFG	MATCH base case simulation and “first guess” used as input to the reanalyzes.
LONGTERM	Reanalysis data set of hourly near-surface ozone concentration covering Sweden and Norway based on 1) the MFG European MATCH simulation and 2) selected hourly near-surface ozone measurements in Sweden and Norway, based on temporal coverage of the measurement sites. Optimal for trend analyses. Analyzed and presented in Sect. 3.
ALL	Reanalysis data set of hourly near-surface ozone concentration covering Sweden and Norway based on 1) the MFG European MATCH simulation and 2) all available Swedish hourly ozone measurements and a selection of the Norwegian (as in LONGTERM). Not used for trend analyses in this study, but best estimate for the hourly near-surface ozone concentration in Sweden at any point in time.
MEUR	MATCH sensitivity simulation where the full domain anthropogenic emissions are kept constant from year to year, set to the level of 2011.
MSE	MATCH sensitivity simulation where the Swedish anthropogenic emissions are kept constant from year to year, set to the level of 2011.
MBC	MATCH sensitivity simulation where the top and lateral boundaries for all species are kept constant from year to year, set to the level of 2011.
MMET	MATCH sensitivity simulation where the meteorology is kept constant, using the meteorological year 2011.

5

6



- 1 Table 1b. Formation of contributions to the linear trend over the period 1990-2013 from the
- 2 sensitivity simulations (Se emis, Eur emis, Bound and Meteo, see Table 1a).

Se emis	Contribution to the trend caused by the change in anthropogenic Swedish emissions, calculated as the model scenario difference: MFG-MSE.
Eur emis	Contribution to the trend caused by the change in anthropogenic European, non-Swedish, emissions, calculated as the model scenario difference: (MFG-MEUR)-(MFG-MSE).
Bound	Contribution to the trend caused by the change in lateral and upper boundaries, calculated as the model scenario difference: MFG-MBC.
Meteo	Contribution to the trend caused by the variation in meteorology, calculated as the model scenario difference: MFG-MMET.
SUM	Sum of the contributions to the trend, calculated as the sum of: Se emis+Eur emis+Bound+Meteo.

3

4



1 Table 2. Evaluation of modelled hourly near-surface ozone concentrations in 2013 at Swedish
 2 observation sites. Mean value (mean), standard deviation (σ), model mean bias normalized by
 3 the observed mean (%bias), Pearson correlation coefficients (r) for data including at least 10
 4 pairs, the root mean square error (RMSE) and number of observed hours at the sites. The
 5 evaluation includes the reanalyzed data sets ALL and LONGTERM, where ALL is evaluated
 6 at the 12 Swedish sites included in that simulation, and LONGTERM is evaluated at the 6
 7 Swedish sites included in that simulation (cf. Fig. 4). For each of these data set evaluations we
 8 include the observation *dependent* reanalysis (2dvar), the observation *independent* cross
 9 validation of the reanalysis (cross) and the MATCH base case simulation (MFG). The top half
 10 of the table shows the temporal performance (spatial mean of statistics, see Supplement Sect.
 11 S1). The bottom half of the table shows spatial performance (spatial statistics of annual
 12 means, see Supplement Sect. S1).

		spatial mean of hourly statistics					
		mean (ppb(v))	std dev (ppb(v))	%bias (%)	r	RMSE (ppb(v))	#hours
ALL	obs	30.9	11.0				8760
	MFG	31.1	9.4	1.4	0.67	8.8	
	cross	30.6	9.9	-0.3	0.76	8.0	
	2dvar	30.8	11.1	-0.6	0.94	3.5	
LONGTERM	obs	32.6	10.5				8760
	MFG	31.2	9.7	-3.3	0.67	8.7	
	cross	32.2	9.3	-0.1	0.72	8.5	
	2dvar	32.6	10.7	0.2	0.97	2.7	
		spatial statistics of annual means					
		mean (ppb(v))	std dev (ppb(v))	%bias (%)	r	RMSE (ppb(v))	#stns
ALL	obs	30.9	2.5				12
	MFG	31.1	1.2	0.6	0.21	3.0	
	cross	30.6	1.8	-1.0	0.11	3.5	
	2dvar	30.8	2.8	-0.5	0.98	0.7	
LONGTERM	obs	32.6	2.2				6
	MFG	31.2	1.0	-4.1	X	3.4	
	cross	32.2	1.6	-1.2	X	4.3	
	2dvar	32.6	2.2	0.2	X	0.2	

13

14



- 1 Table 3. Linear trend during 1990-2013 of policy related metrics in the 3 Swedish regions
- 2 North, Central and South (cf. Fig. 3). Stars (*, **, and ***) indicate that the trend is
- 3 significant ($p \leq 0.05$, $p \leq 0.01$, $p \leq 0.001$, respectively).

Metrics	North	Central	South
Mean [$\mu\text{g m}^{-3} \text{ year}^{-1}$]	+0.18*	+0.13	+0.18*
SOMO35 [ppb(v) d year^{-1}]	+14	-3.1	-4.7
Maximum 8h mean [$\mu\text{g m}^{-3} \text{ year}^{-1}$]	-0.11	-0.68**	-1.2**
Maximum 1h mean [$\mu\text{g m}^{-3} \text{ year}^{-1}$]	-0.14	-0.82**	-1.4***
AOT40c [ppm(v) h year^{-1}]	-0.01	-0.07*	-0.09
AOT40f [ppm(v) h year^{-1}]	+0.03	-0.09	-0.12*
#hours $> 80 \mu\text{g m}^{-3}$ [# year^{-1}]	+26*	+1.7	+6.6
#days $> 70 \mu\text{g m}^{-3}$ [# year^{-1}]	+1.3	+0.73	+1.1
#days $> 120 \mu\text{g m}^{-3}$ [# year^{-1}]	+0.01	-0.12*	-0.32**

4